Supporting Information for:

Generation and Oxidative Reactivity of a Ni(II) Superoxo Complex via Ligand-Based Redox Non-Innocence

Andrew J. McNeece, Kate A. Jesse, Jiaze Xie, Alexander S. Filatov, and John S. Anderson*

Department of Chemistry, The University of Chicago, Chicago, Illinois 60637, United States

*Correspondence to: jsanderson@uchicago.edu

Table of Contents:

Experimental:

General Considerations: All reagents were purchased from commercial suppliers and used without further purification unless otherwise specified. The *t*-butyl hydrazine was synthesized by deprotonating *t*-butyl hydrazine hydrochloride All manipulations were carried out under an atmosphere of N_2 using standard Schlenk and glovebox techniques. Glassware was dried at 180 °C for a minimum of two hours and cooled under vacuum prior to use. Solvents were dried on a solvent purification system from Pure Process Technology and stored over 4 Å molecular sieves under N_2. Tetrahydrofuran was stirred over NaK alloy and run through an additional activated alumina column prior to use to ensure dryness. Solvents were tested for H_2O and O_2 using a standard solution of sodium-benzophenone ketyl radical anion. C_6D_6 was dried by passage over a column of activated alumina and stored over 4 Å molecular sieves in the glovebox. ^1H and $^{13}C\{^1H\}$ spectra were recorded on Bruker DRX 400 or 500 spectrometers. Chemical shifts are reported in ppm units referenced to residual solvent resonances for ^1H and $^{13}C\{^1H\}$ spectra, UV-vis spectra were recorded on a Thermo Evolution 300 spectrometer and addition of gases was performed by injecting via syringe into a cuvette sealed with a septum. UV-visible spectra at elevated temperature were done using a Unisoku Cryostat. IR was recorded on a Bruker Tensor II. EPR spectra were recorded on an Elexsys E500 Spectrometer with an Oxford ESR 900 X-band cryostat and a Bruker Cold-Edge Stinger and were simulated using the Easyspin suite in Matlab software.[1] GC/MS was collected on an Agilent SQ GCMS with 5977A single quad MS and 7890B GC. Elemental analysis was performed by Midwest Microlabs. Electrochemical measurements were performed using a BAS Epsilon potentiostat and analyzed using BAS Epsilon software version 1.40.67NT. Cyclic voltammetry measurements were made using a glassy carbon working electrode, platinum wire counter electrode, and silver wire pseudo-reference electrode, and referenced to internal Fc/Fc^+.

X-Ray Structure Determination

Crystal Structure Determination. The diffraction data were measured at 100 K on a Bruker D8 VENTURE with PHOTON 100 CMOS detector system equipped with a Mo-target micro-focus X-ray tube (λ = 0.71073 Å). Data reduction and integration were performed with the Bruker APEX3 software package (Bruker AXS, version 2015.5-2, 2015). Data were scaled and corrected for absorption effects using the multi-scan procedure as implemented in SADABS (Bruker AXS, version 2014/5, 2015, part of Bruker APEX3 software package). The structure was solved by the dual method implemented in SHELXT[2] and refined by a full-matrix least-squares procedure using OLEX23[3] software package (XL refinement program version 2014/7[4]). Suitable crystals were mounted on a cryo-loop and transferred into the cold nitrogen stream of the Bruker D8 Venture diffractometer. Most of the hydrogen atoms were generated by geometrical considerations and constrained to idealized geometries and allowed to ride on their carrier atoms with an isotropic displacement parameter related to the equivalent displacement parameter of their carrier atoms. Compound **1** was modeled for three component disorder of one of the p-tol rings. Compound **2** was modeled for two component disorder of the bridging triflate group.

X-ray Absorption Measurements.

Powder samples were prepared by grinding finely. A Teflon washer (5.3 mm internal diameter) was sealed on one side with Kapton tape and powder was then transfer transferred to the inside of this ring before compacting with a Teflon rod and sealing the remaining face with Kapton tape. All sample preparation was performed under an inert atmosphere. X-ray absorption near-edge spectra (XANES) and Extended Absorption Fine Structure (EXAFS) were employed to probe the local environment around Ni. Data were acquired at the Advanced Photon Source at Argonne National Laboratory with a bending magnet source with ring energy at 7.00 GeV. Ni K-edge (8332.8 eV) data were acquired at the MRCAT 10-BM beam line in transmission. The incident, transmitted and reference X-ray intensities were monitored using gas ionization chambers. A metallic nickel foil standard was used as a reference for energy calibration and was measured simultaneously with experimental samples. X-ray absorption spectra were collected at room temperature.

Data collected was processed using the Demeter software suite by extracting the EXAFS oscillations $\chi(k)$ as a function of photoelectron wavenumber k. The theoretical paths were generated using FEFF6 and the models were determined using the fitting program Artemis.[5]

Synthesis of 2,5-bis((2-*t*-butylhydrazono)(*p*-tolyl)methyl)-pyrrole) (^{tBu,Tol}DHP•2HCl). In the glovebox, 500 mL 3-neck round bottom flask equipped with two septa and a reflux condenser was charged with 2,5-ditolylacylpyrrole[6] (3.0 g 9.9 mmol), *t*-butyl hydrazine (6.1 g, 70 mmol, 7.0 eq), toluene (250 mL), molecular sieves, catalytic 2 M HCL etherate (0.01 mL) and a stir bar. This was removed from the glovebox and refluxed on the Schlenk line for 5 days at 115 °C. The resulting yellow solution was cooled to room temperature, returned to the glovebox, and filtered through Celite to remove the molecular sieves, giving a clear yellow solution. This was evaporated to dryness to give an orange oil, which was taken up in benzene, then 2 M hydrogen chloride in diethyl ether (10 mL, 2 eq) was added, resulting in precipitation of a yellow solid. The yellow solid was collected by filtration, then the benzene filtrate was evaporated to dryness, taken up in petroleum ether (100 mL) and filtered to collect more yellow solid. The two batches of solid were combined to give ^{tBu,Tol}DHP•2HCl (3.4 g, 6.6 mmol, 66%). ^{1}H NMR ($CDCl_3$, 500 MHz, 25° C) δ = 12.96 (s, 1H, N-H pyrrole), 11.46 (s, 4H, N-H hydrazone), 7.63 (d, 4H, J = 8 Hz, tol C-H), 7.27 (d, 4H, J = 8 Hz, tol C-H), 6.48 (d, 2H, J = 4 Hz, Pyrrole C-H), 2.46 (s, 6H, tol-Me), 1.71 (s, 18H, *t*bu). ^{13}C {^{1}H} NMR ($CDCl_3$, 125 MHz 25 °C) δ = 164.6 (C=N), also 142.6, 133.3, 129.9, 128.8, 126.9, 119.8, 62.5, 25.3, 21.3. IR (nujol mull, cm^{-1}): 3457 (m, N-H), 3131 (m, N-H), 3088 (m, N-H), 1598 (s, C=N). Anal calcd: C 65.1, H 7.6, N 13.5 Found: C 65.8, H 7.7, N 11.8

Synthesis of [^{tBu,Tol}DHP$^{\bullet}$]Ni (1). To a stirring THF solution of ^{tBu,Tol}DHP•2HCl (0.47 g, 0.92 mmol, 40 mL) was added 2.5 M *n*-BuLi in hexanes (1.5 mL, 4 eq), turning from yellow to red. The red mixture was stirred for 5 minutes, then added to a stirring slurry of $NiCl_2$DME in THF, turning deep purple. After stirring overnight for 12 hours, all volatiles were removed under vacuum, and the resulting purple residue was taken up in benzene and passed through a silica plug, then evaporated to give **1** as a purple powder. Yield: 0.20 g, 0.40 mmol, 43%. Single crystals can be obtained by crystallization from concentrated Et_2O at –35° C. EPR (frozen toluene/petroleum ether, 15 K, g_z, g_x, g_y) 2.24, 2.10, 2.07. Evans method (C_6D_6, 25 °C, μ_B) μ_{eff} = 2.02. IR (KBr pellet, cm^{-1}) 3026 (w), 2963 (s), 2919 (s), 1905, 1797, 1521 (s, C=N), 1466, (m) 1460 (s), 1364 (s), 1011 (m), 820 (s), 719 (m) UV-vis (Benzene solution) 275 nm, 570 nm, 800 nm. Anal calcd: C 67.3; H 6.8; N 14.0. Found: C 66.5; N 7.6; H 13.7.

Synthesis of [^{tBu,Tol}DHP]NiOTf (2). To a stirring THF solution of **1** (0.050 g, 0.1 mmol, 5 mL) was added a THF solution of AgOTf (0.026 g, 0.1 mmol, 2 mL, 1 eq) resulting in an immediate color change from dark purple to dark blue. The reaction was stirred for 30 min, then filtered and the solvent was evaporated. The resulting blue residue was washed with petroleum ether (5 mL) then taken up in benzene (10 mL), filtered, and evaporated to give **2** as a blue powder (0.052 g, 0.08 mmol, 80%). Single crystals could be obtained by layering a toluene solution of **2** with petroleum ether at -35 °C. ^{1}H NMR (C_6D_6, 500 MHz, 25° C) δ = 46.06, 14.13, 12.54, 12.40, -1.36. IR (KBr Pellet, cm^{-1}) 2973 (s), 2920 (m), 2867 (w). 1614 (m), 1508 (m), 1468 (m) 1366 (s), 1261 (vs), 1174 (s) 1100 (m), 1032 (m), 822 (w). Anal Calc'd C 53.7; H 5.2; N 10.8. Found: C 53.8; H 5.6; N 10.6

Synthesis of [^{tBu,Tol}DHP]NiO$_2$ (3). A solution of **1** in benzene (0.023 g, 0.046 mmol, 5 mL) was removed from the glovebox and air was bubbled through the solution for 30 seconds, resulting in a color change from purple to red. All volatiles were removed under vacuum, giving **3** as a red oil. Yield: 0.022 g, 0.041 mmol, 90%. EPR (frozen benzene, 15 K, g_z, g_x, g_y) 2.23, 2.09, 2.00. Evans method (C_6D_6, 25 °C, μ_B) μ_{eff} = 1.65. IR (KBr Pellet, cm^{-1}) 2965 (s), 2919 (m), 2861 (m), 1607 (m), 1512 (m), 1440 (s), 1361 (s), 1303 (m), 1266 (s), 1183 (m), 1115 (m), 1103 (m), 1014 (s), 833 (m), 805 (m). UV-vis (Benzene solution) 350 nm, 550 nm, 870 nm. ESI-MS (MeCN solution): m/z = 539.2 [^{tBu,Tol}DHP]Ni(NCMe)$^{+}$. Due to decomposition of the material over time, satisfactory elemental analysis could not be obtained.

Synthesis of 3 by reaction of 2 with KO$_2$. To a stirring THF solution of **2** (0.013 g, 0.02 mmol, 3 mL) was added a THF slurry of KO_2 (0.0015 g, 0.02 mmol, 1 mL, 1 eq). This was stirred for 1 hour, slowing turning from deep blue to dark red. The solution was filtered and evaporated under vacuum to give **3** as a red oil.

Oxidation of benzyl alcohol. In a nitrogen glovebox, to a solution of **1** in C_6D_6 (0.005 g, 0.01 mmol, 0.5 mL) was added benzyl alcohol (0.002 mg, 0.02 mmol, 2 eq) and naphthalene (6 mg). This was added to an NMR tube and removed from the glovebox and exposed to air, turning from purple to red as **1** reacted to form **3**. The tube was resealed and heated to 50 °C for 5 hours and the appearance of 1.9 equivalents of benzaldehyde was observed by integration against the internal naphthalene standard. The rate of the reaction was tracked via UV-Vis on a 1 mM solution of **3**, and monitored at 550 nm. The absorbance was fit as a non-linear curve to determine the rate constant of the reaction, where the final absorbance was also fit as a variable.

Oxidation of toluene. To 5 mL of toluene was added **1** (0.005 g, 0.01 mmol), which was then removed from the glovebox, exposed to air to convert the **1** to **3**, resealed under air, and then heated to 70 °C for 3 hours, at which point it was tested by GC/MS and the resulting benzaldehyde peak was integrated versus a benzaldehyde standard curve and indicated the formation of 0.9 equivalents of benzaldehyde.

Oxidation of PPh$_3$. To a C_6D_6 solution of **1** (0.003 g, 0.006 mmol, 0.5 mL) was added PPh_3 (0.030 g, 0.012 mmol, 20 eq) and removed from the glovebox, exposed to air overnight, then tested by ^{31}P NMR. The amount of PPh_3O was quantified by integration compared to the PPh_3 peak to give the percentage of the PPh_3 that had converted indicating the formation of 2.0 equivalents of

PPh_3O. An identical experiment using **3** under N_2 also converted PPh_3 to $PPh_3{=}O$, and control experiments with PPh_3 under air in the absence of **3** did not show oxidation under the same timescale.

Reaction of 3 with DPH. To a stirring C_6D_6 solution of **3** (0.010 g, 0.019 mmol, 1 mL) was added freshly recrystallized DPH (0.007 g, 0.037 mmol, 1.9 eq) and stirred at room temperature in the glovebox. After 10 minutes the reaction was sampled via NMR and showed the appearance of 0.6 equiv of azobenzene, indicating slow H-atom transfer reactivity.

Reaction of 3 with DHA. To a stirring C_6D_6 solution of **3** (0.010 g, 0.019 mmol, 1 mL) was added freshly recrystallized DHA (0.004 g, 0.022 mmol, 1.1 eq) and stirred at room temperature in the glovebox overnight. Monitoring by NMR and GC/MS indicated no change to the DHA.

II. NMR Spectra

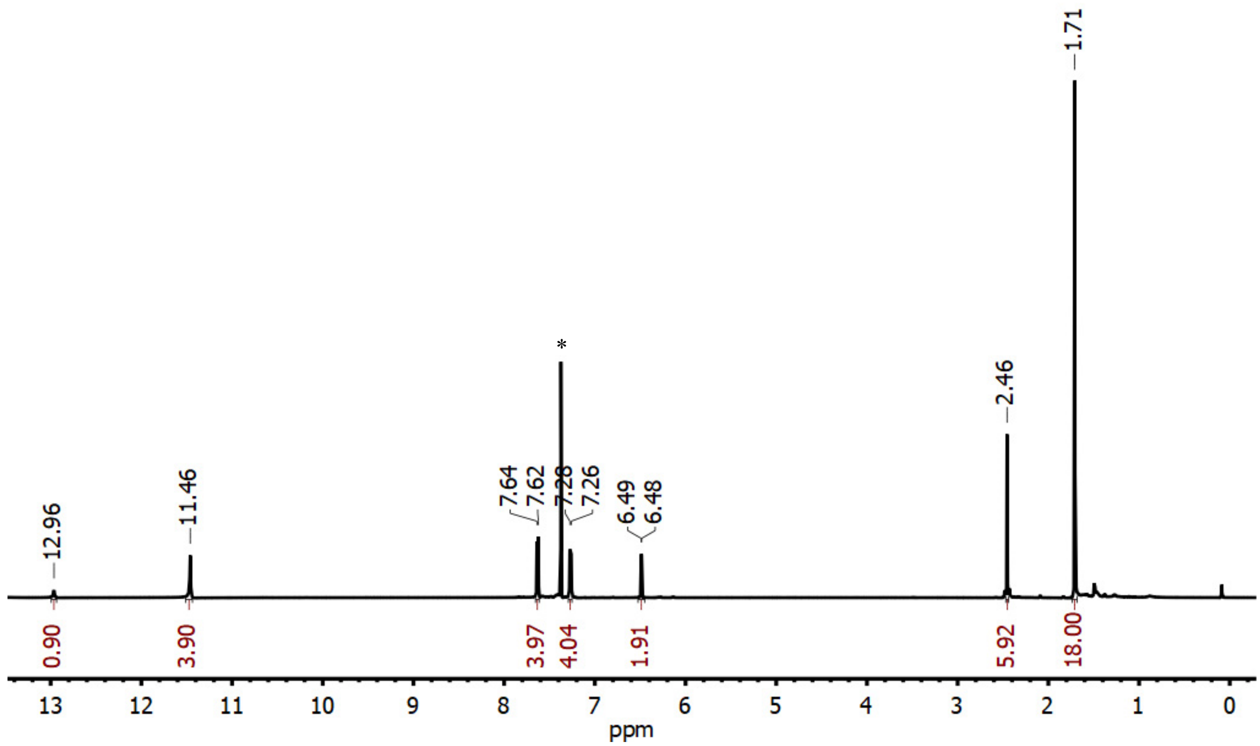

Figure S1 [1]H NMR of ^{tBu,Tol}DHP•2HCl in $CDCl_3$ *residual benzene

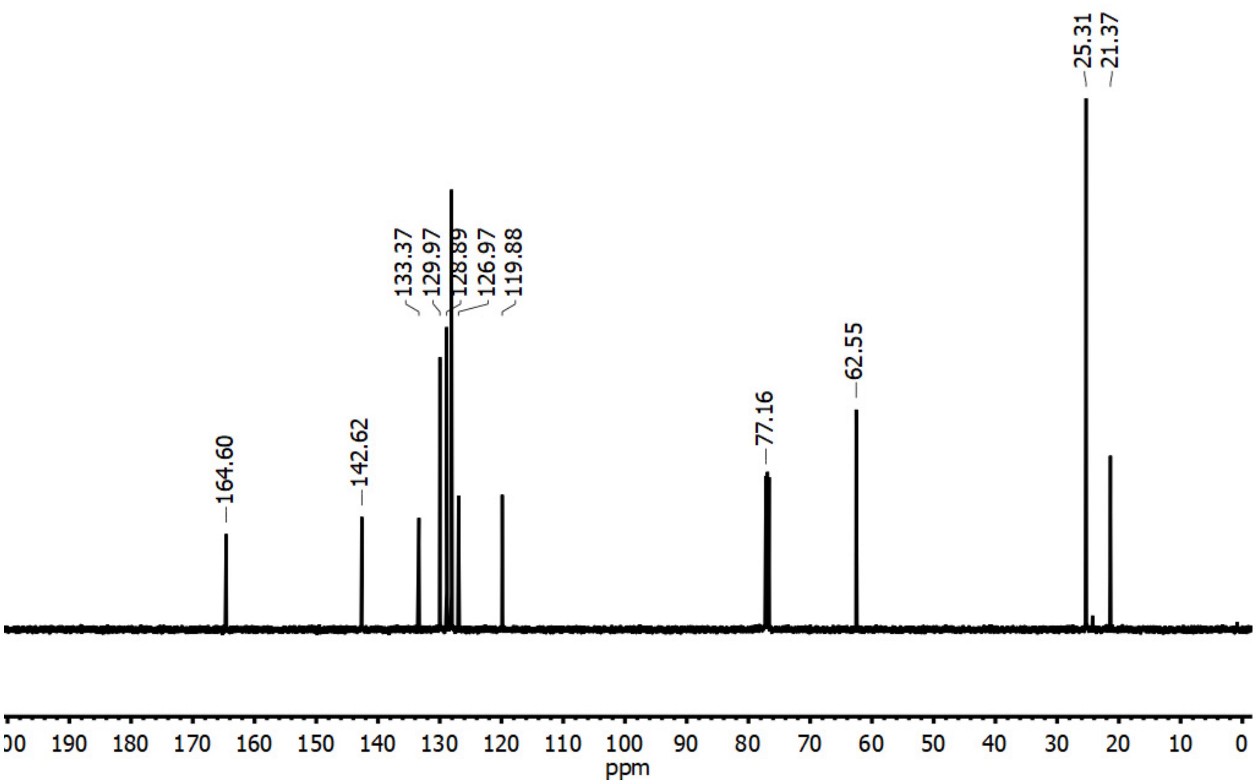

Figure S2. $^{13}C\{^{1}H\}$ NMR of ^{tBu,Tol}DHP•2HCl in $CDCl_3$

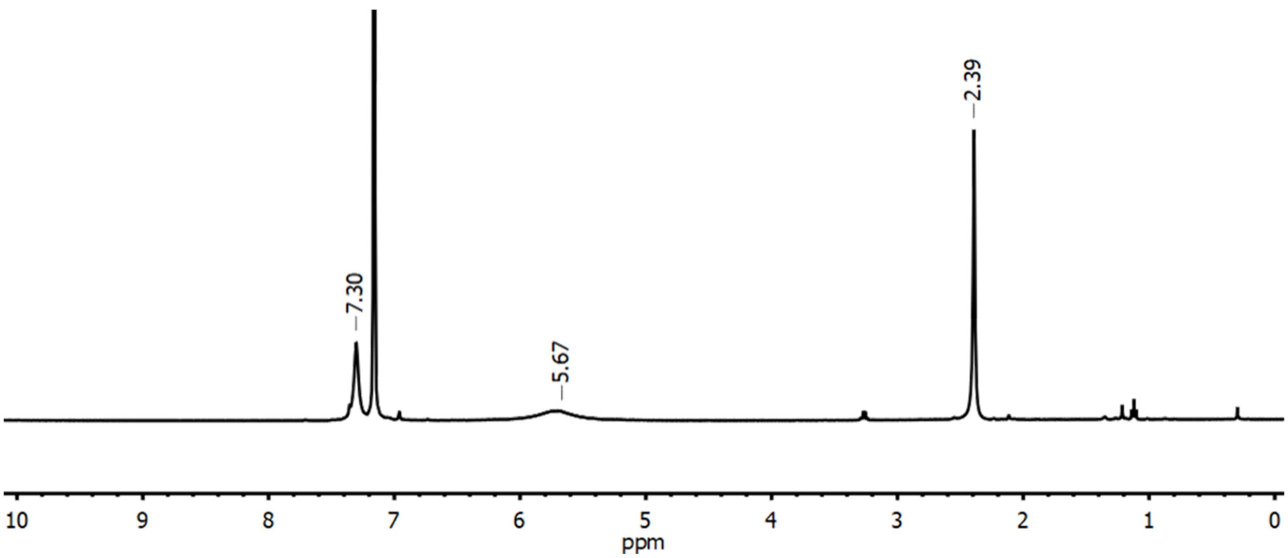

Figure S3. ^1H NMR of **1** in C_6D_6

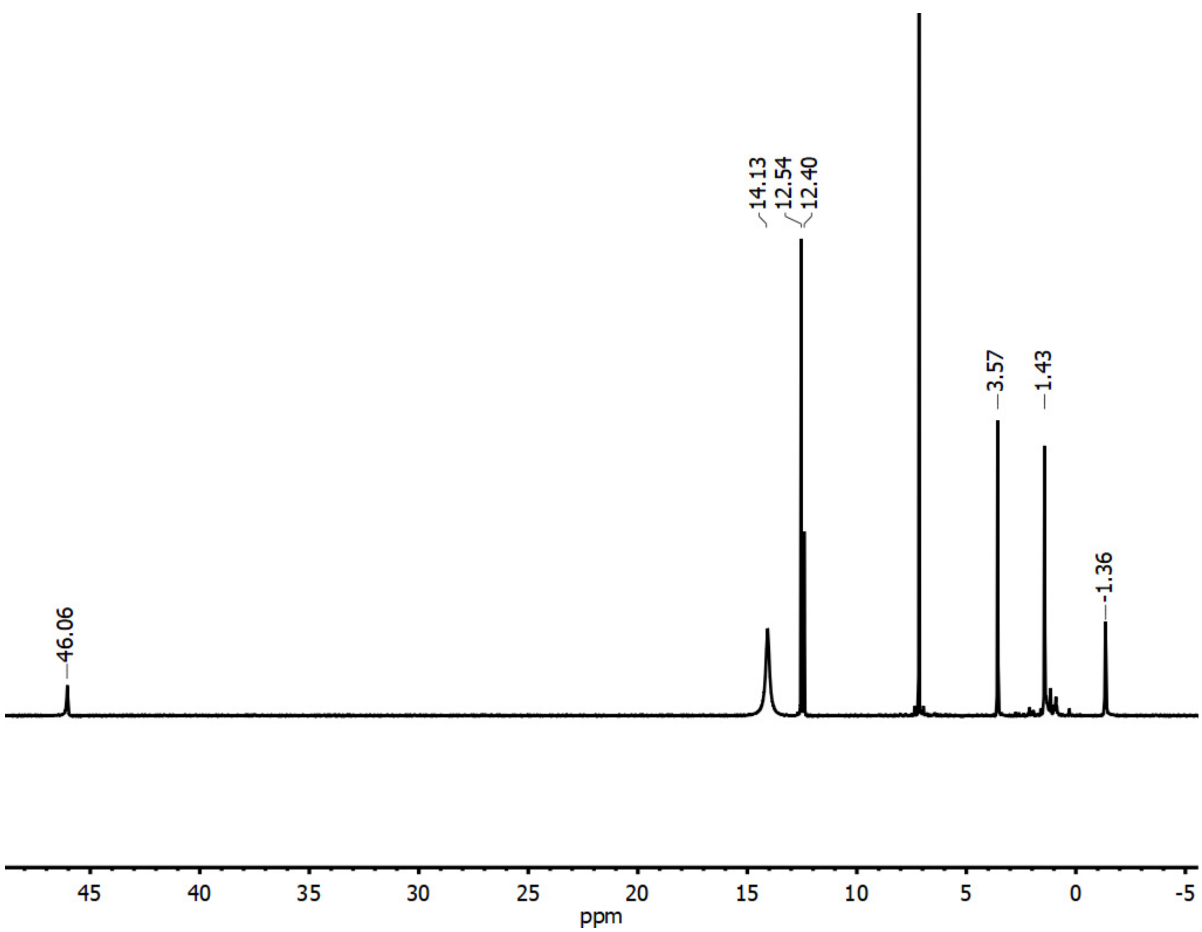

Figure S4. ^1H NMR of **2** in C_6D_6

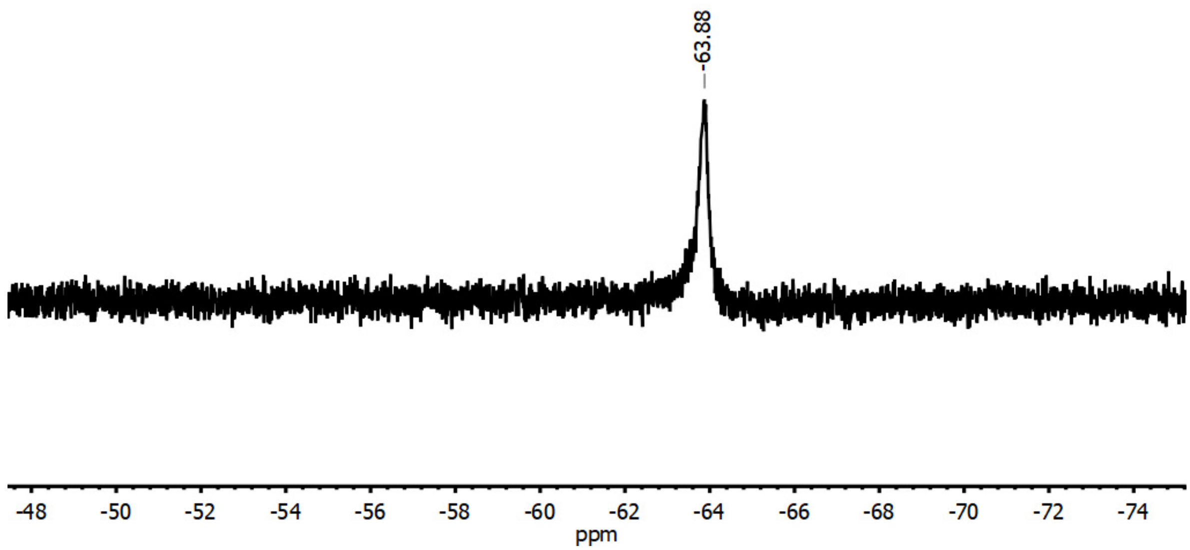

Figure S5. ^{19}F NMR of **2** in C_6D_6

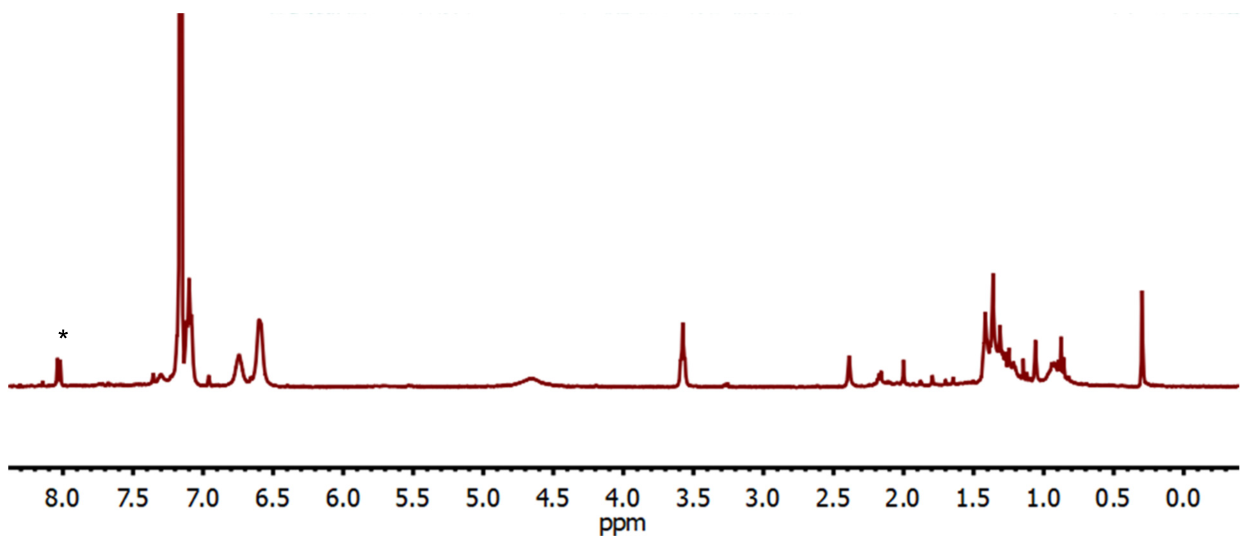

Figure S6. ^{1}H NMR of the reaction of **3** with DPH in C_6D_6 after 10 minutes. *Azobenzene

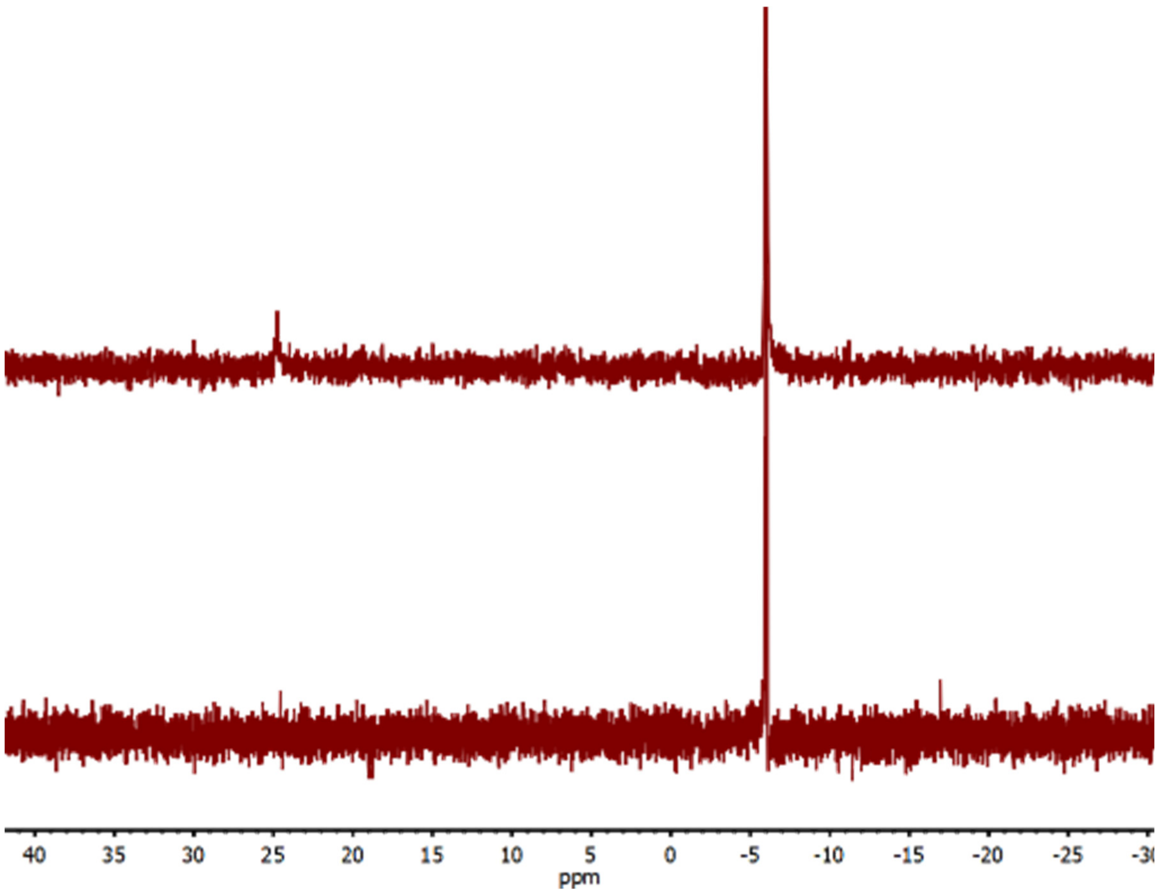

Figure S7. Top: reaction of **3** under air with 20 eq PPh_3 showing conversion to PPh_3O. PPh_3O was quanitified by percent conversion based on integration of the PPh_3 and PPh_3O peaks. Bottom: Control reaction of PPh_3 under air showing no conversion.

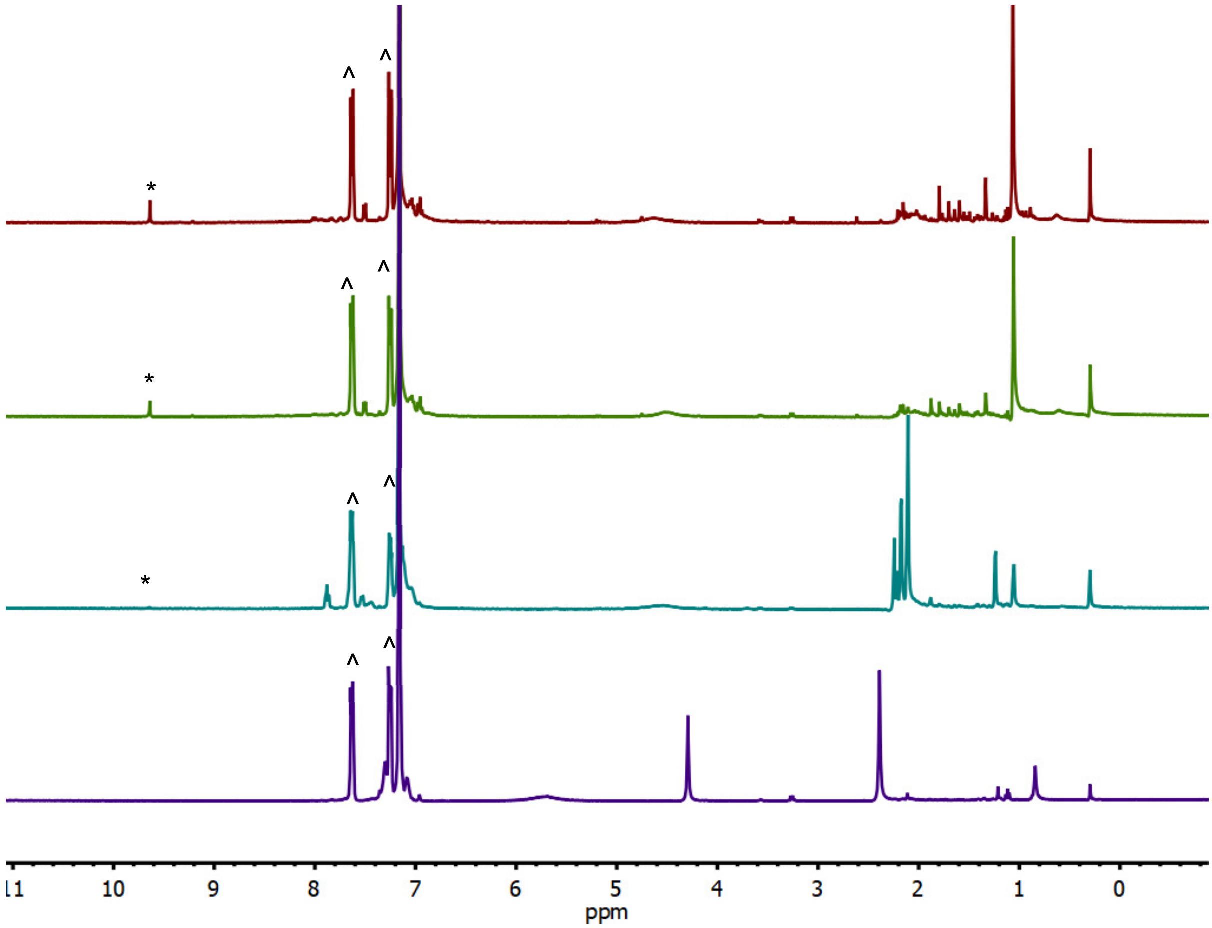

Figure S8. [1]H NMR of conversion of benzyl alcohol to benzaldehyde by **3**. Bottom: t = 0, each NMR after is at 1.5 hour time points. *Benzaldehyde. ^Napthalene

.

III. EPR Spectra

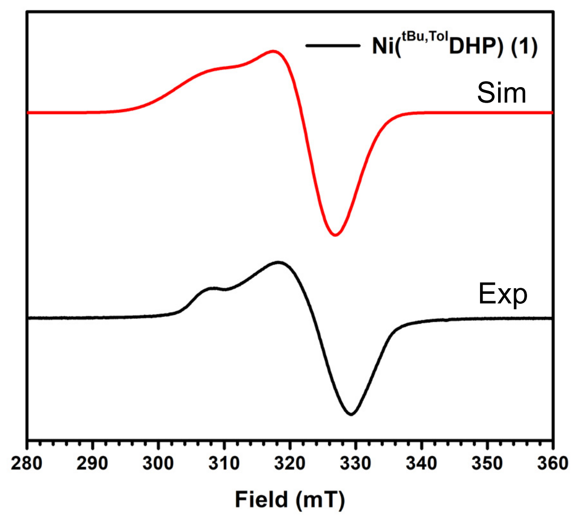

Figure S9. X-band EPR of 1 mM **1 1** in toluene/petroleum ether at 15 K, MW frequency = 9.628 GHz, MW power = 2.0 mW. Simulation parameters: g = 2.24, 2.12, 2.12, HStrain = 400, 275, 275 Hz

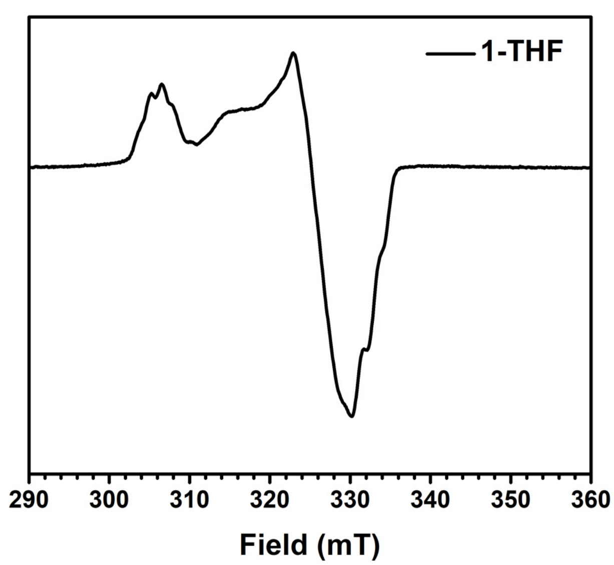

Figure S10. X-band EPR of 1 mM **1** in frozen THF at 15 K. MW power = 2 mW, MW freq = 9.630

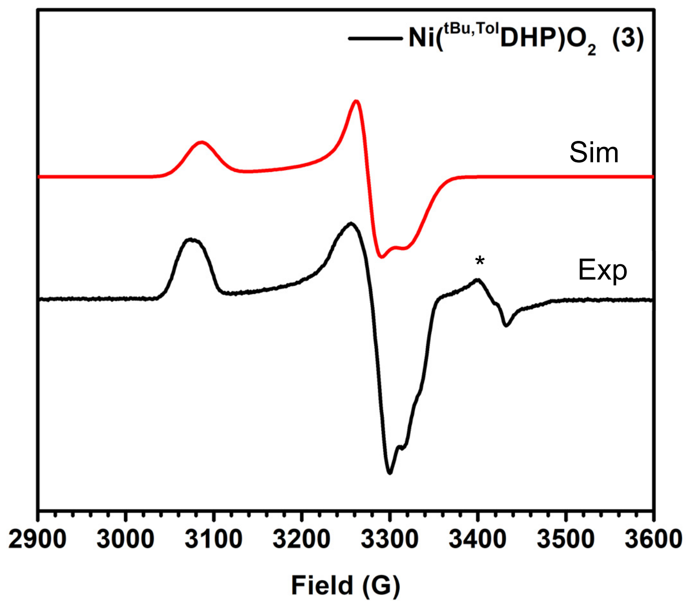

Figure S11. X-Band EPR of 10 mM **3** in THF at 15 K, MW frequency = 9.631 GHz, MW power = 0.06 mW. Simulation parameters: g = 2.23, 2.10, 2.07. HStrain = 125, 70, 130 Hz. *S = ½ impurity

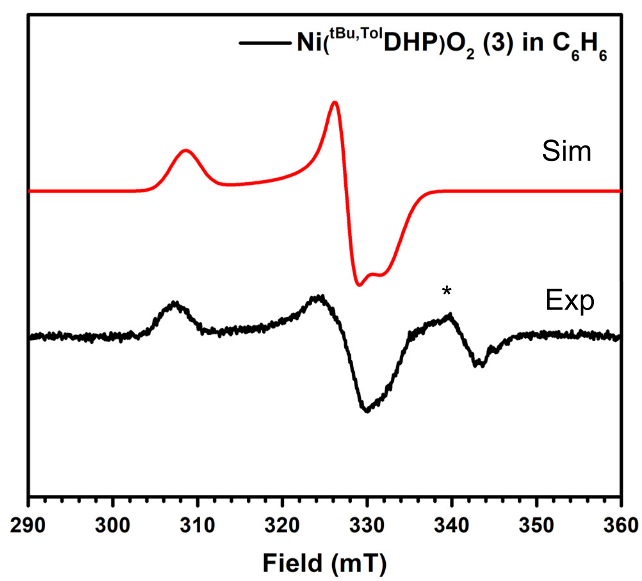

Figure S12. X-Band EPR of 1 mM **3** in benzene at 15 K. MW frequency = 9.629 GHz, MW power = 2.0 mW. Simulation parameters: g = 2.23, 2.10, 2.07. HStrain = 125, 70, 130 Hz. *S = ½ impurity

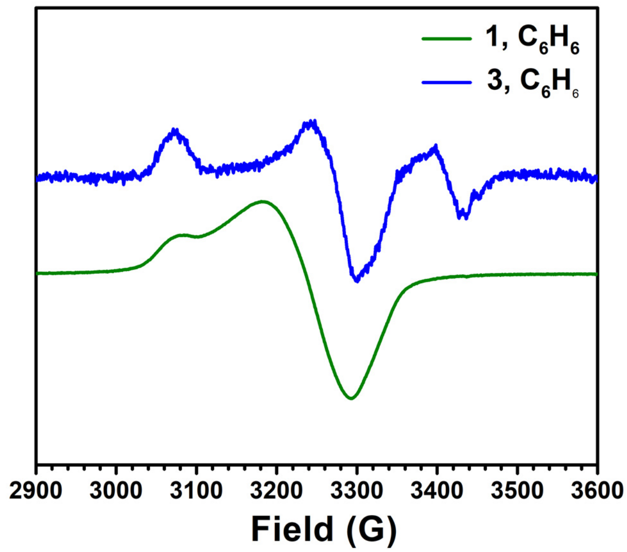

Figure S13. Comparison of the EPR of **1** and **3** in benzene. Intensities have been normalized for comparison.

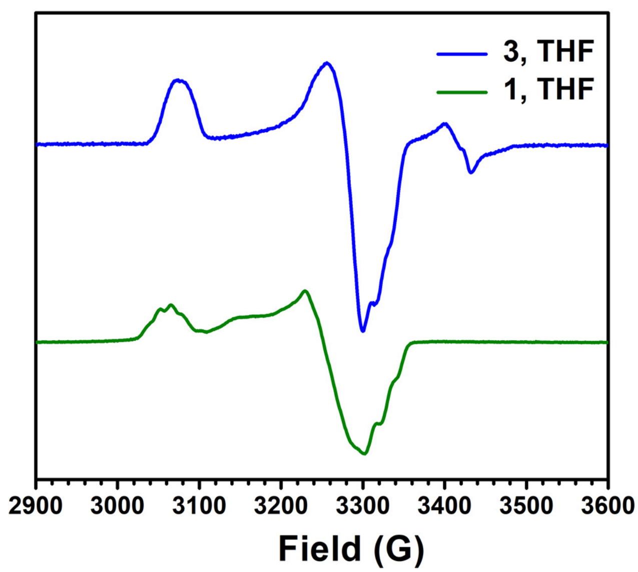

Figure S14. Comparison of the EPR of **1** and **3** in THF. Intensities have been normalized for comparison.

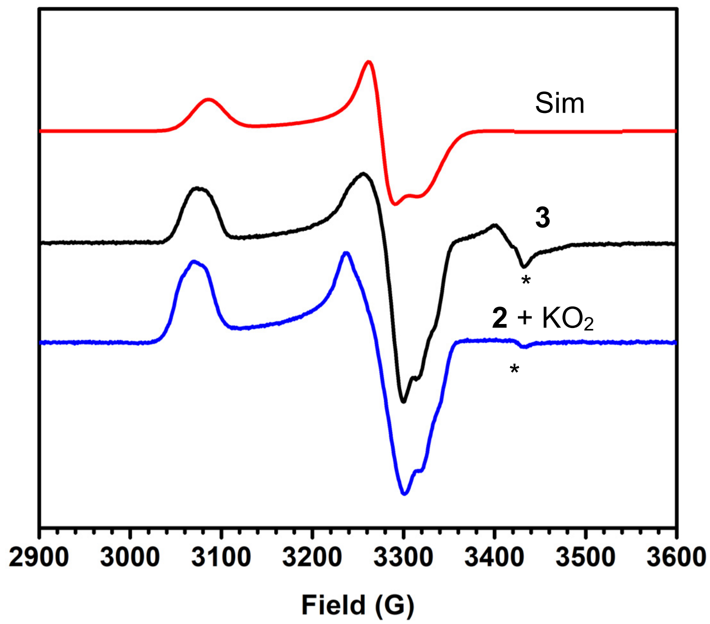

Figure S15. X-band EPR of **3** in frozen THF compared with EPR of **3** generated from **2** at 15 K. MW power = 0.002 mW, MW freq = 9.630. *S = ½ impurity. Intensities have been normalized for comparison

IV. UV-visible Spectra

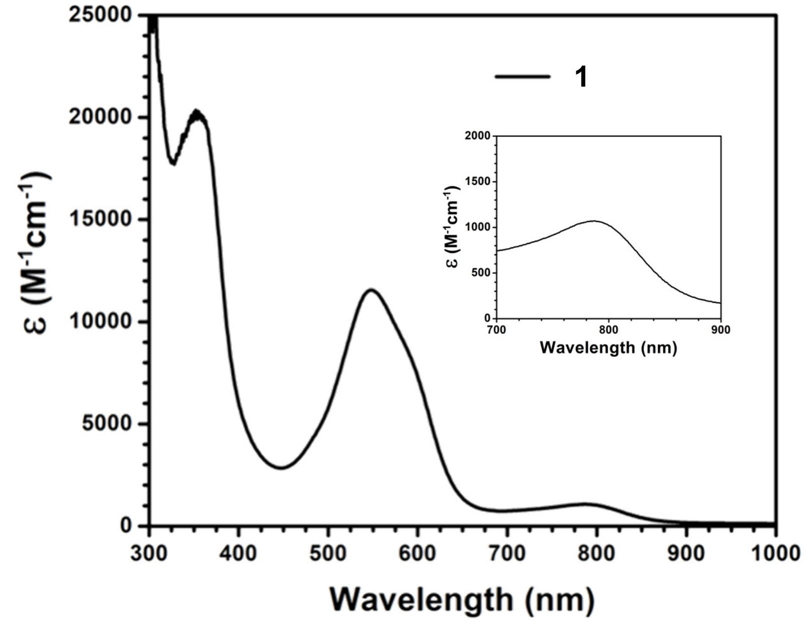

Figure S16. UV-visible spectrum of 0.5 mM **1** in benzene at room temperature, with an inset of the low energy feature

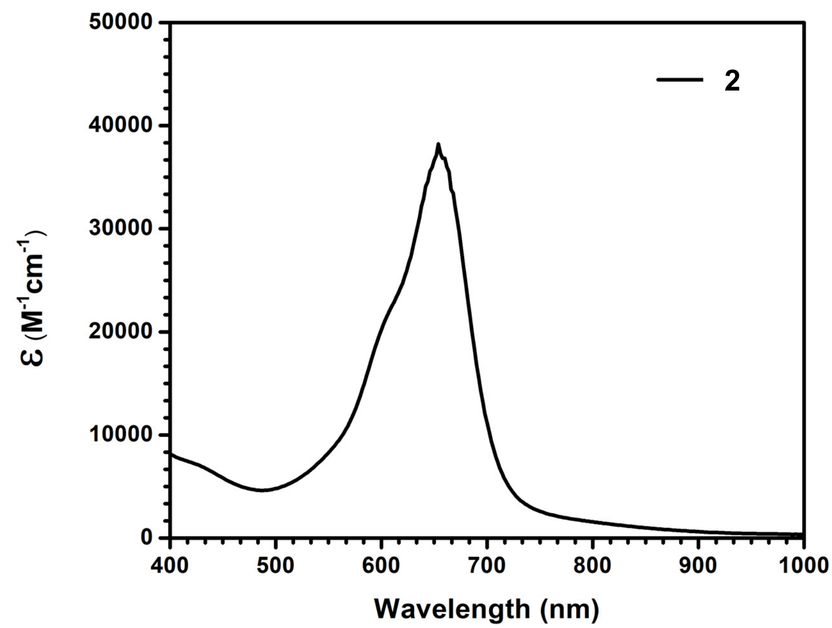

Figure S17. UV-visible spectra of 0.25 mM **2** in THF at room temperature

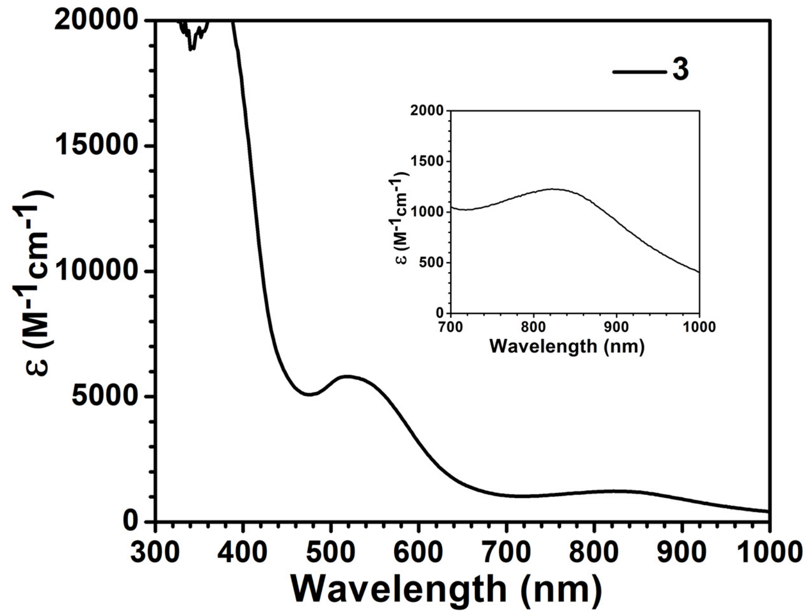

Figure S18. UV-visible spectrum **3** (1 mM in Ni) in benzene at room temperature, with an inset of the low energy feature

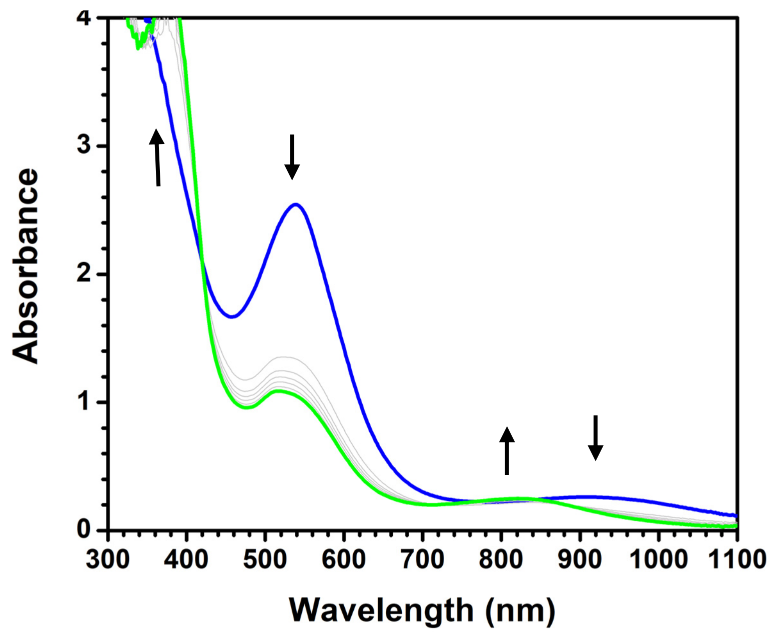

Figure S19. UV-visible spectra of conversion of 0.5 mM **1** to **3** in benzene after injection of an excess of ambient air, with scans taken every 52 seconds. The feature at 400 nm is cut off due to overloading the detector

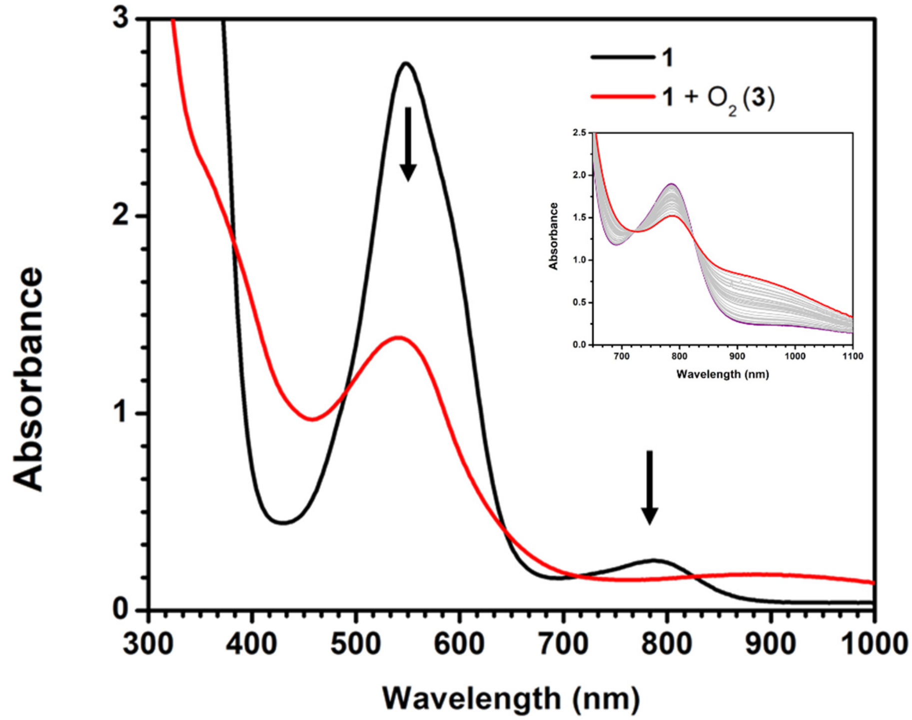

Figure S20. Conversion of 0.5 mM **1** to **3** by exposure of **1** to O_2 at room temperature in THF, with an inset showing isosbestic conversion at the low energy feature, with scans every 15 seconds. Note that the low energy feature exhibits some solvent dependence compared to Figure S18, as it shifts to lower energy in THF

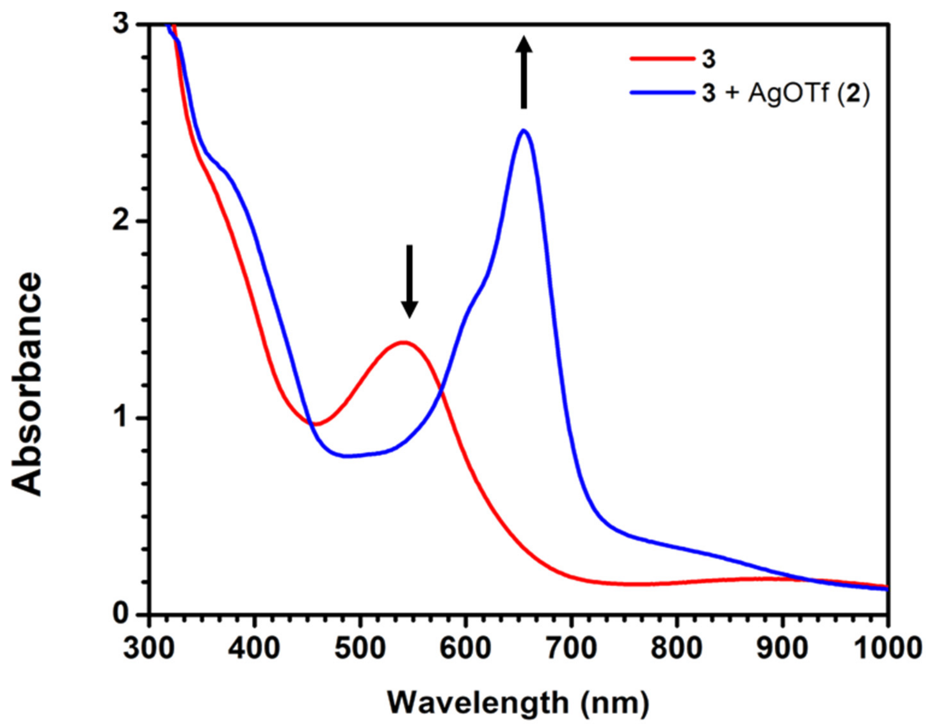

Figure S21. Conversion of **3** (0.5 mM in Ni) to **2** by addition of AgOTf at room temperature in THF

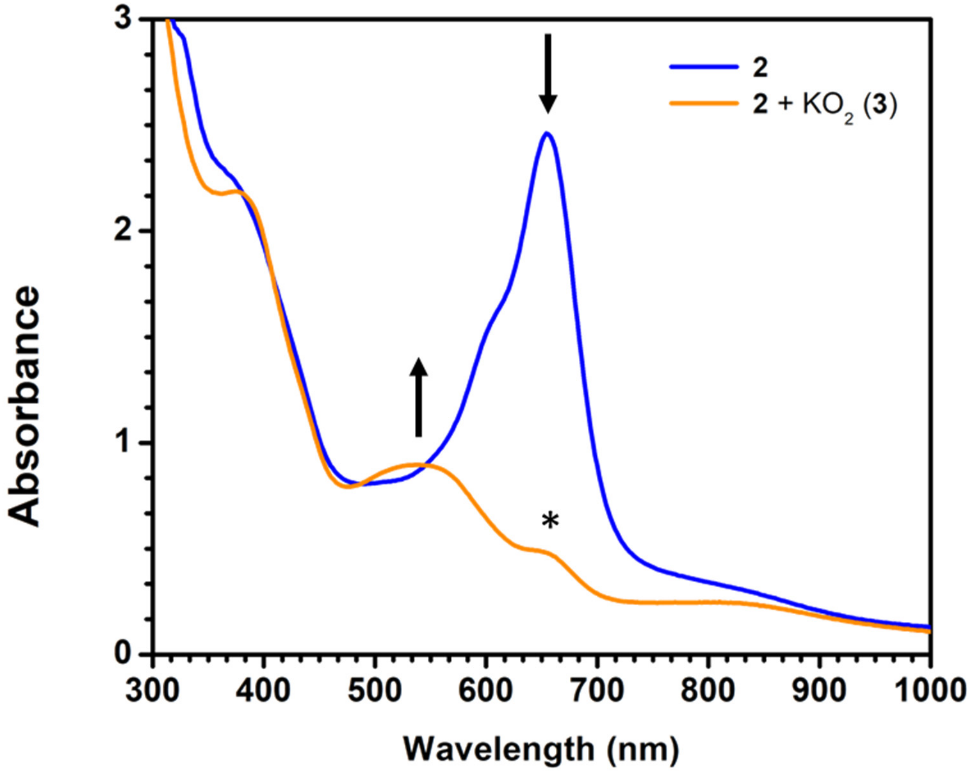

Figure S22. Conversion of 0.1 mM **2** to **3** with KO_2 at room temperature in THF. *The feature at 650 nm is residual **2** that has not fully reacted

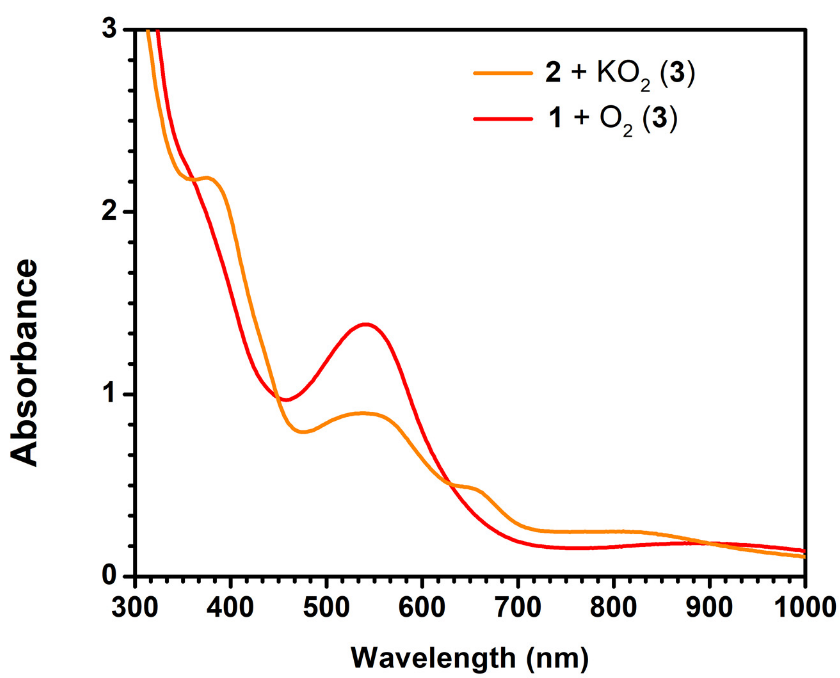

Figure S23. UV-Vis comparison of **3** generated via two different methods. The presence of residual **2** is responsible for the extra features in the orange spectrum.

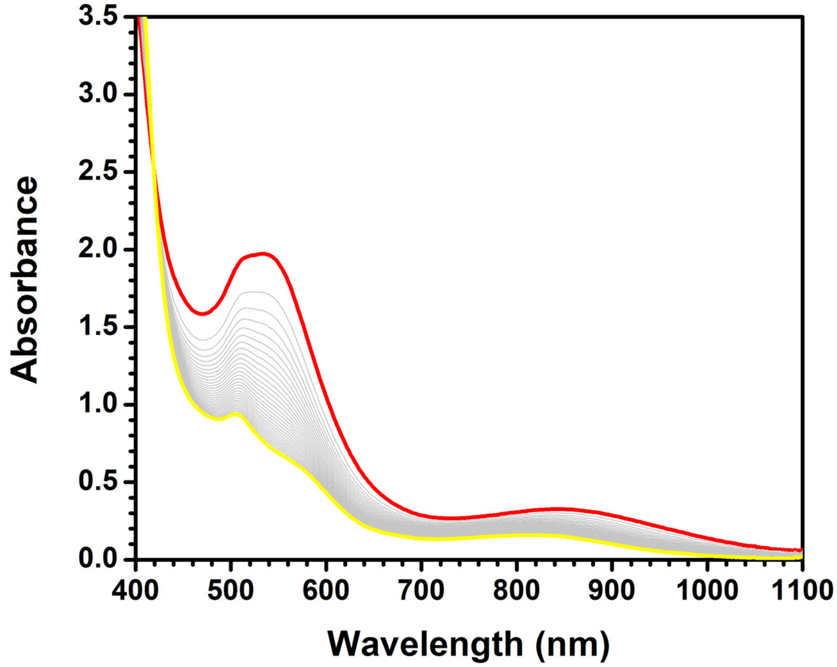

Figure S24. Left: UV-visible spectra of the reaction of **3** with benzyl alcohol (30 eq) in benzene at 50°C in C_6H_6 with scans every 2 minutes.

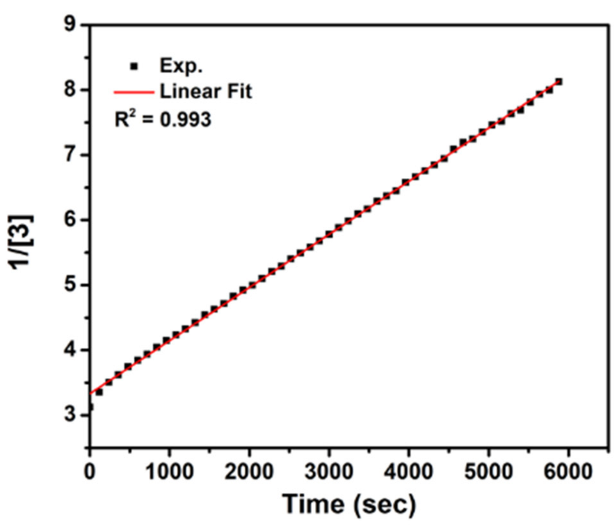

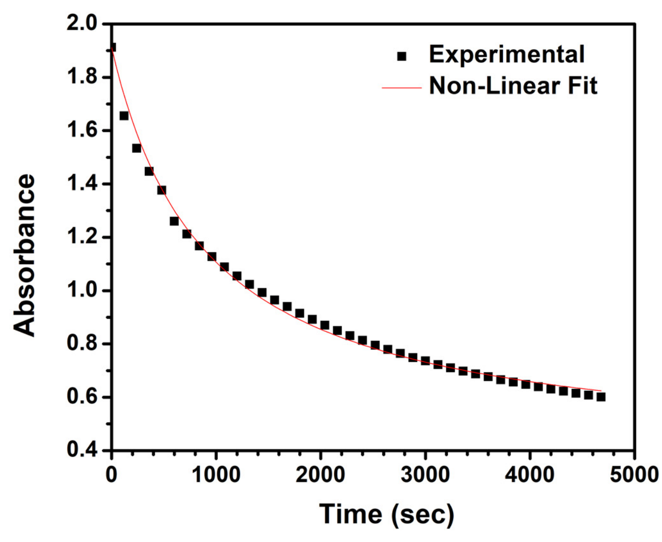

Figure S25. Linear fit to 1/[3] (left) and non-linear fit of absorbance vs. time (right). Rate constant from non-linear fit: -0.0011 sec^{-1} The data was fit to $A = A_{inf} + (A_0 - A_{inf})/(1+KT)$. R^2 of Fit: 0.99

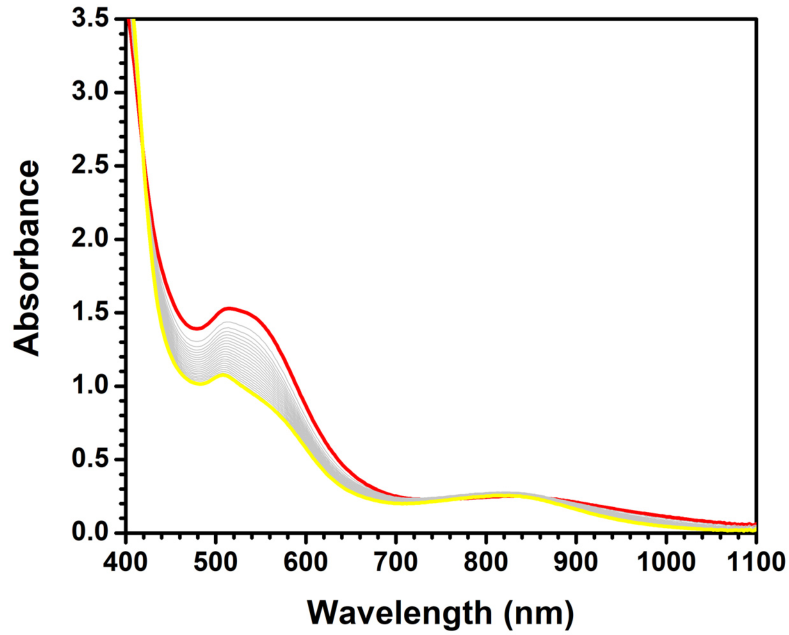

Figure S26. UV-visible spectra of decay of **3** at 50° C in benzene, with scans taken every 2 minutes

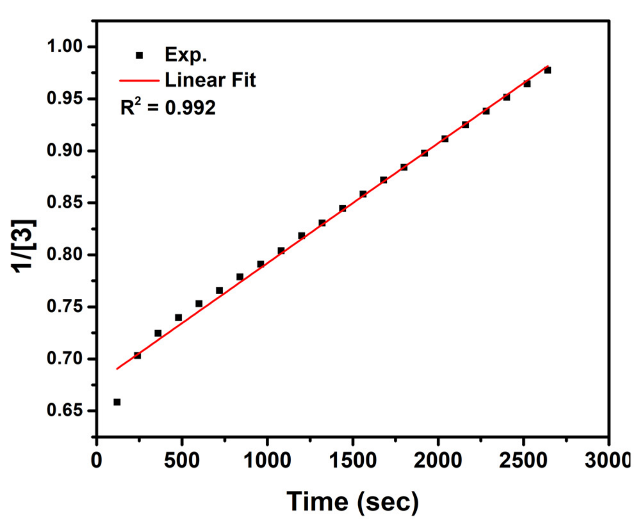

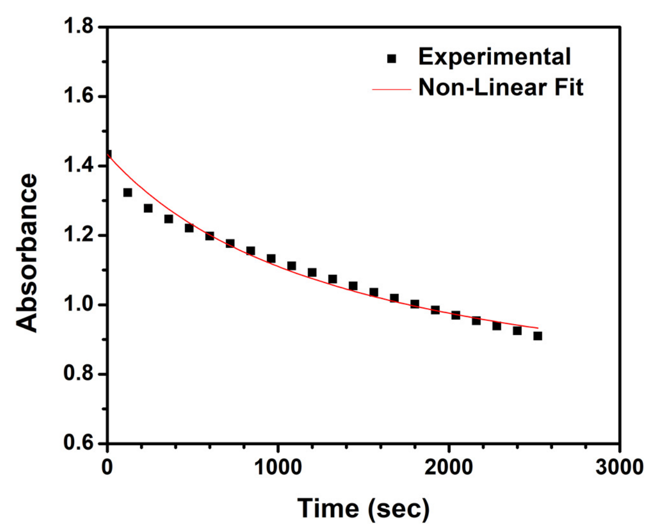

Figure S27. Linear fit to 1/[3] (left) and non-linear fit of absorbance vs. time (right) Rate constant from non-linear fit: 6.9 x 10^{-4}. The data was fit to $A = A_{inf} + (A_0 - A_{inf})/(1+KT)$. R^2 of fit: 0.97

V. Electrochemistry

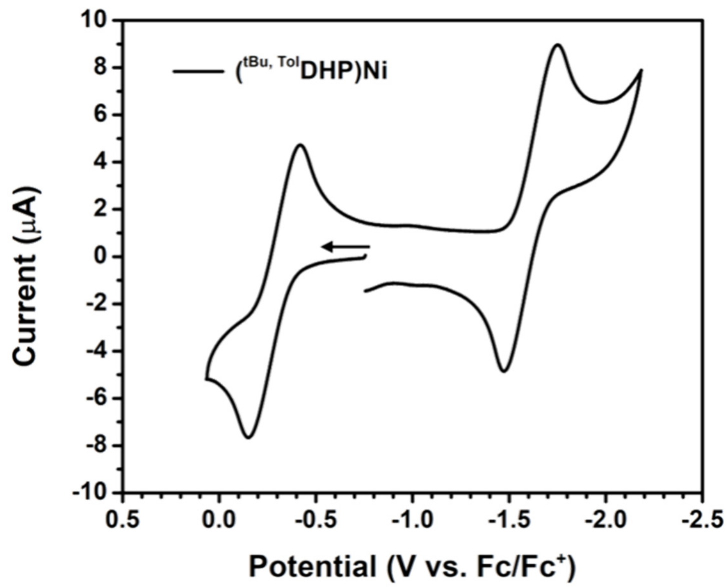

Figure S28. Cyclic voltammogram of 1 mM **1** in 0.1 M NBu_4PF_6 in THF with 100 mV/sec scan rate

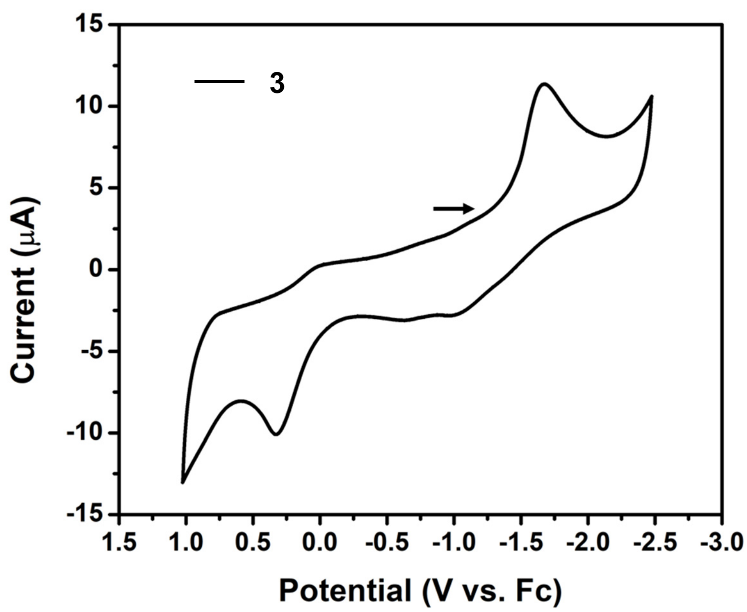

Figure S29. Cyclic voltammogram of 1 mM **3** in 0.1 M NBu_4PF_6 in THF with 100 mV/sec scan rate

VI. IR Spectra

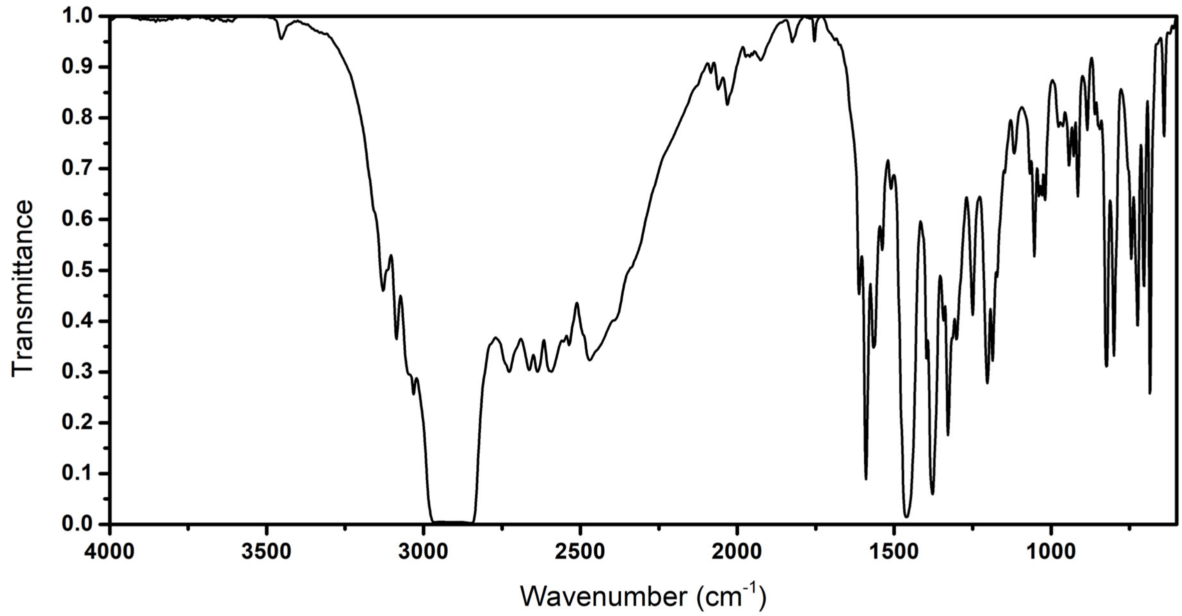

Figure S30. IR (nujol mull) of ^{tBu,Tol}DHP•2HCl. The intense features from 3000-2500 cm^{-1} and 1500 cm^{-1} are from the nujol.

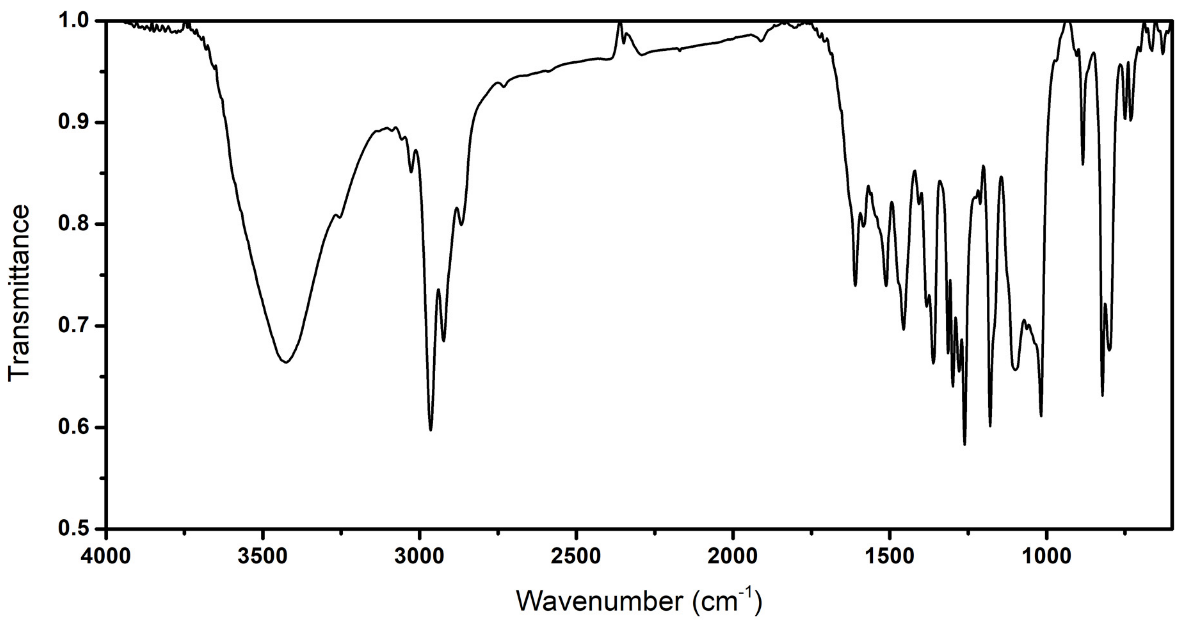

Figure S31. IR (KBr Pellet) of **1**. The broad feature at 3500 cm^{-1} is due to residual water in the KBr

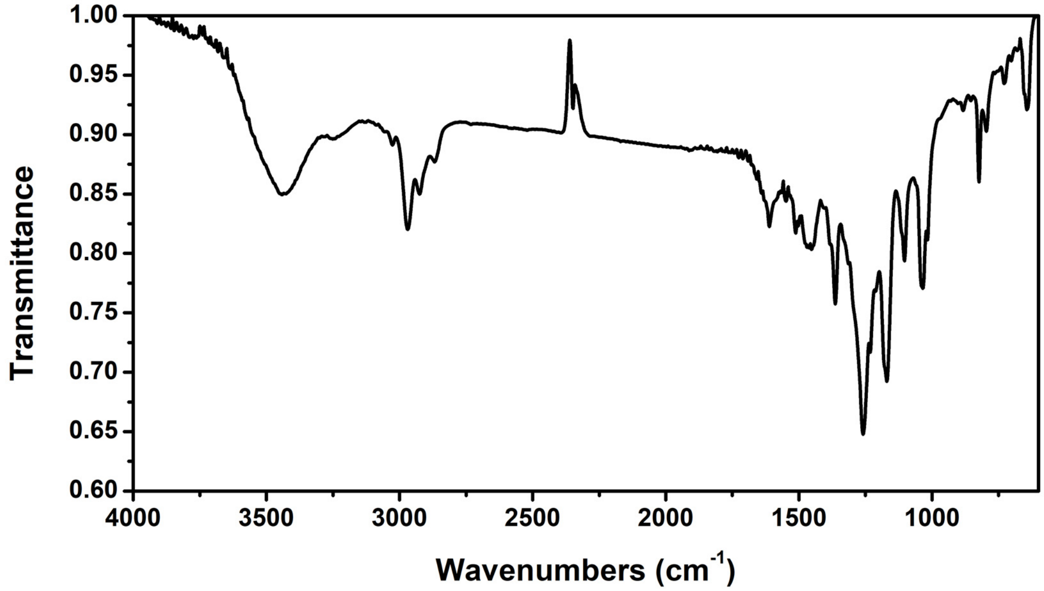

Figure S32. IR (KBr Pellet) of **2**. The broad feature at 3500 is due to residual water in the KBr

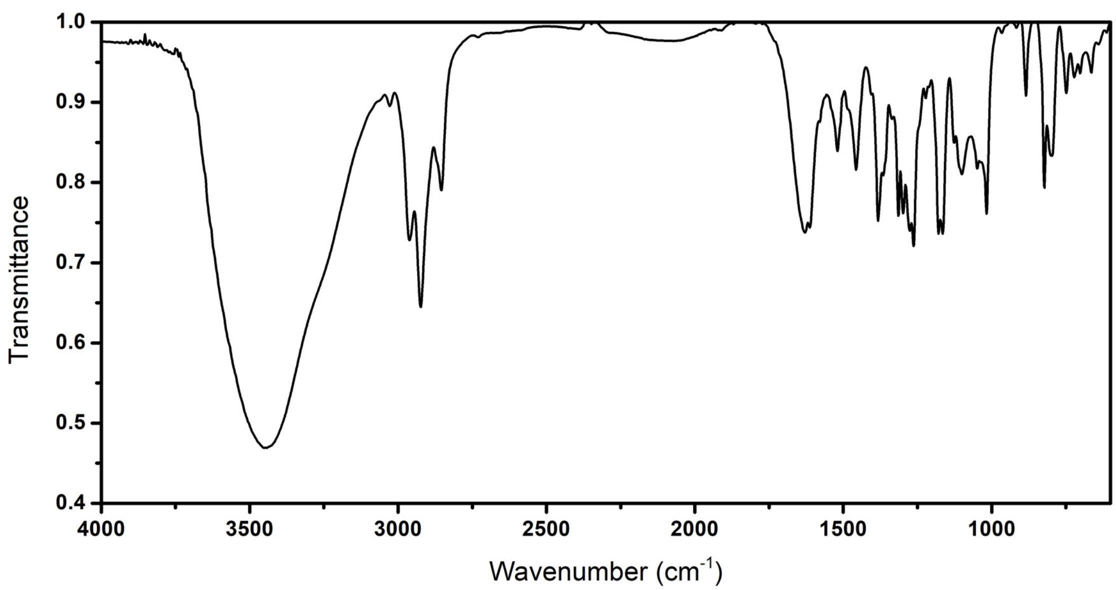

Figure S33. IR (KBr Pellet) of **3**. The broad feature at 3500 is due to residual water in the KBr

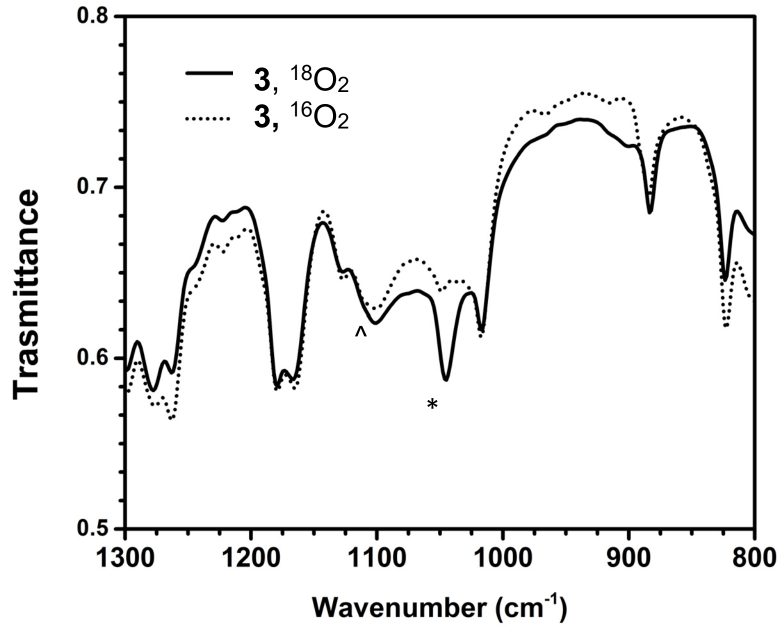

Figure S34. IR (KBr Pellet) of **3** with ^{16}O (dotted line) overlaid with the IR (KBr Pellet) of **3** with ^{18}O (solid line). Predicted shift: 64 cm^{-1} Actual: 60 cm$^{-1.}$ *Isotopically enhanced feature. ^presumed ^{16}O stretch. Note that there is overlap from other vibrations in this region.

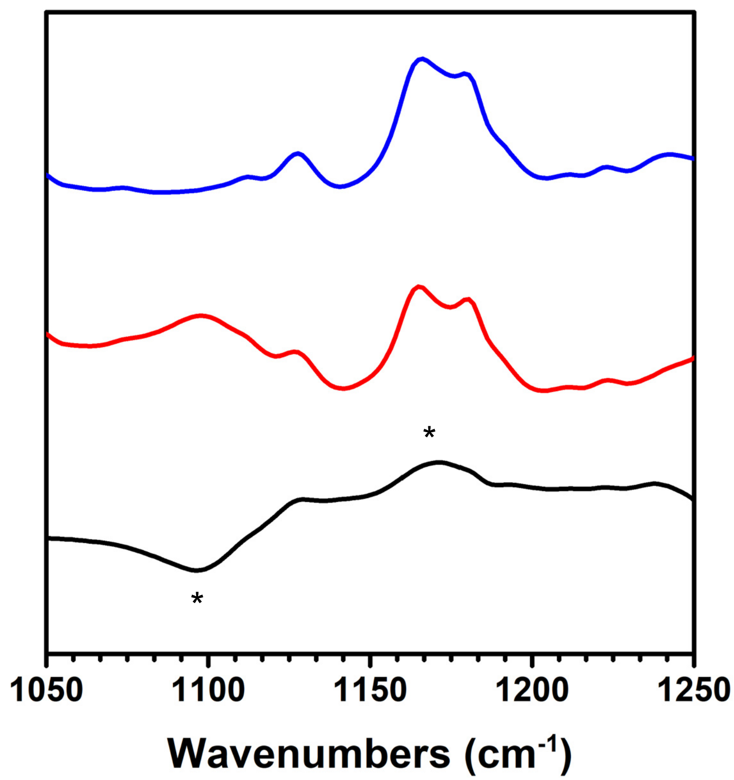

Figure S35. IR (Benzene solution) of **3** with $^{16}O_2$ (top), $^{18}O_2$ (middle), and the subtraction (bottom). Predicted Shift: 68 cm$^{-1+.}$ Actual: 73 cm^{-1} *Isotopically shifted feature at 1170 and 1097 cm^{-1}

VII. GC/MS

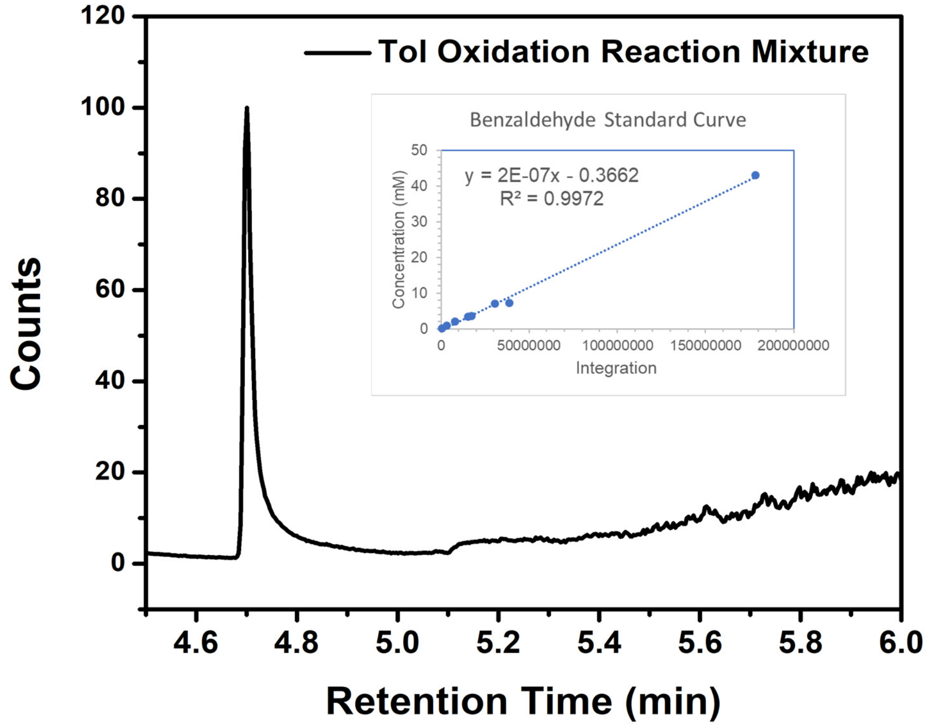

Figure S36. GC trace of oxidation of toluene with **3** showing appearance of benzaldehyde at 4.7 minutes. Inset: Calibration curve for benzaldehyde

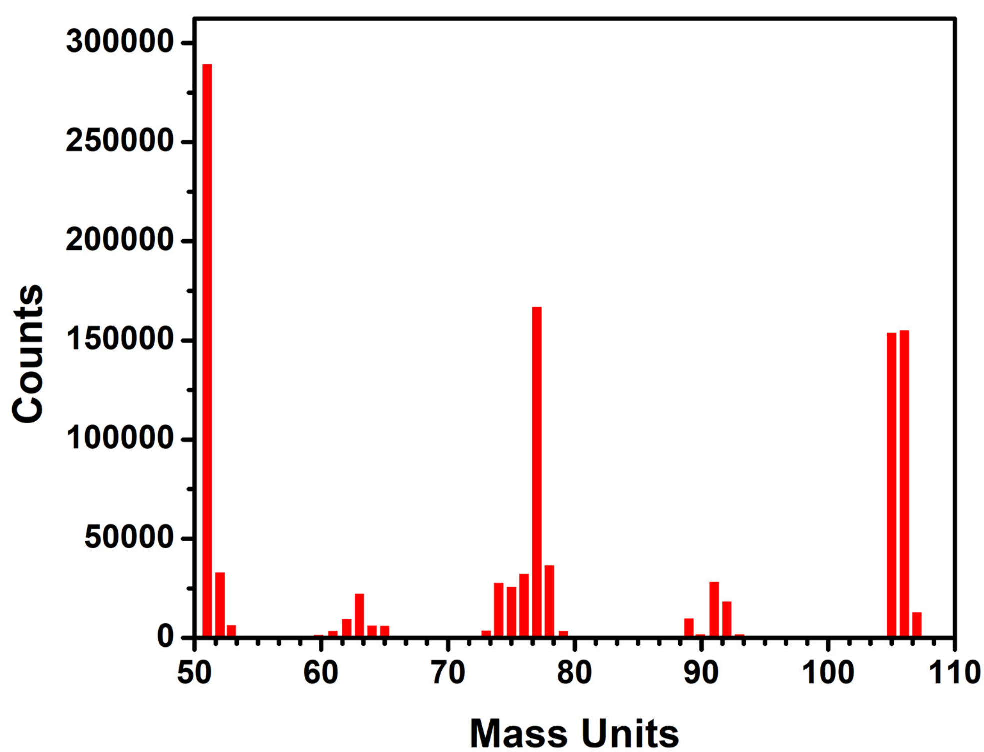

Figure S37. MS of benzaldehyde from oxidation of toluene by **3**

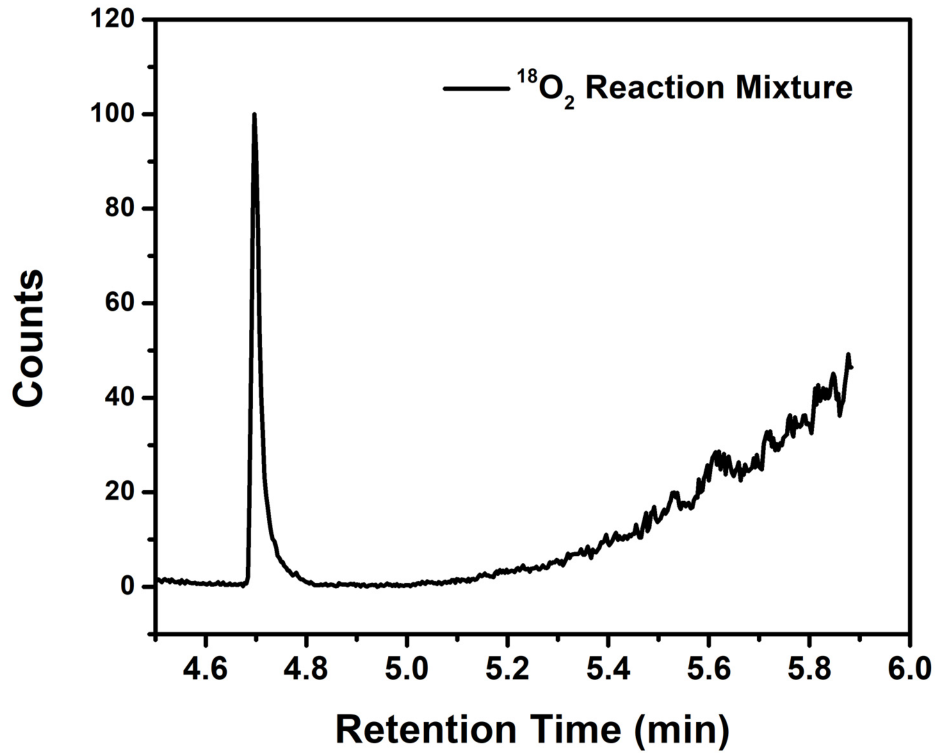

Figure S38. GC trace of reaction of **3** with toluene under $^{18}O_2$

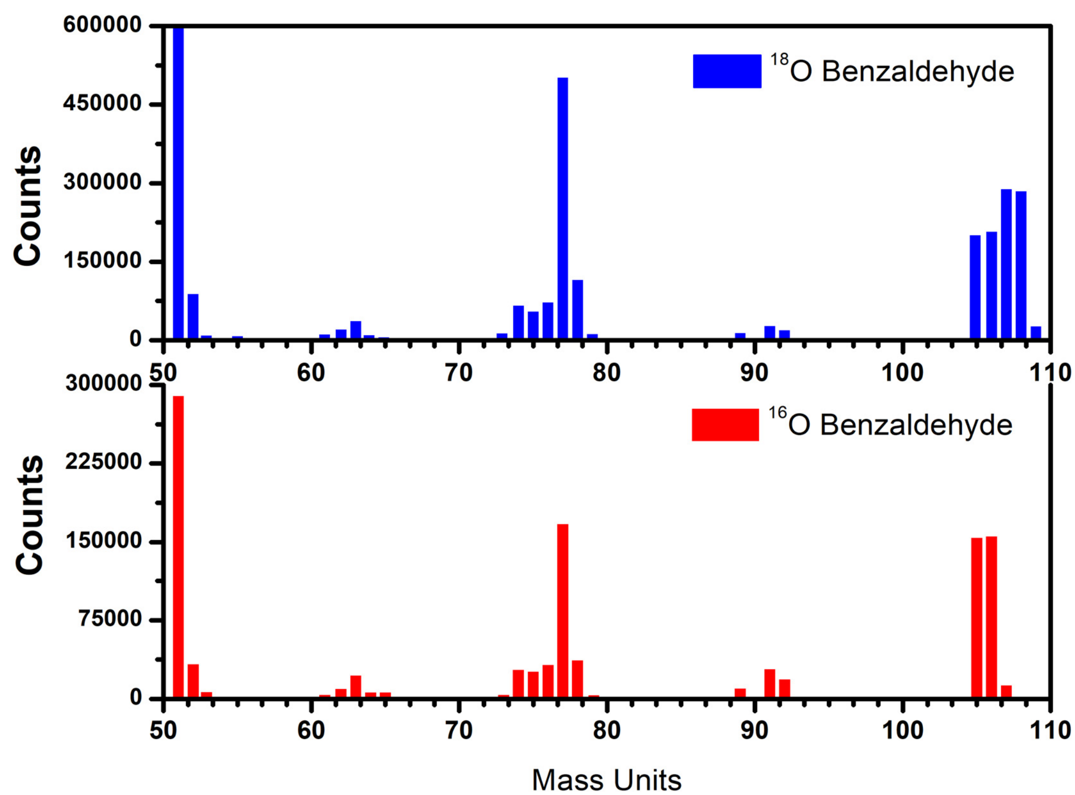

Figure S39. MS comparison between ^{16}O benzaldehyde and ^{18}O enriched benzaldehyde from toluene oxidation. Residual ^{16}O benzaldehyde is from exchange with natural abundance water in the reaction.

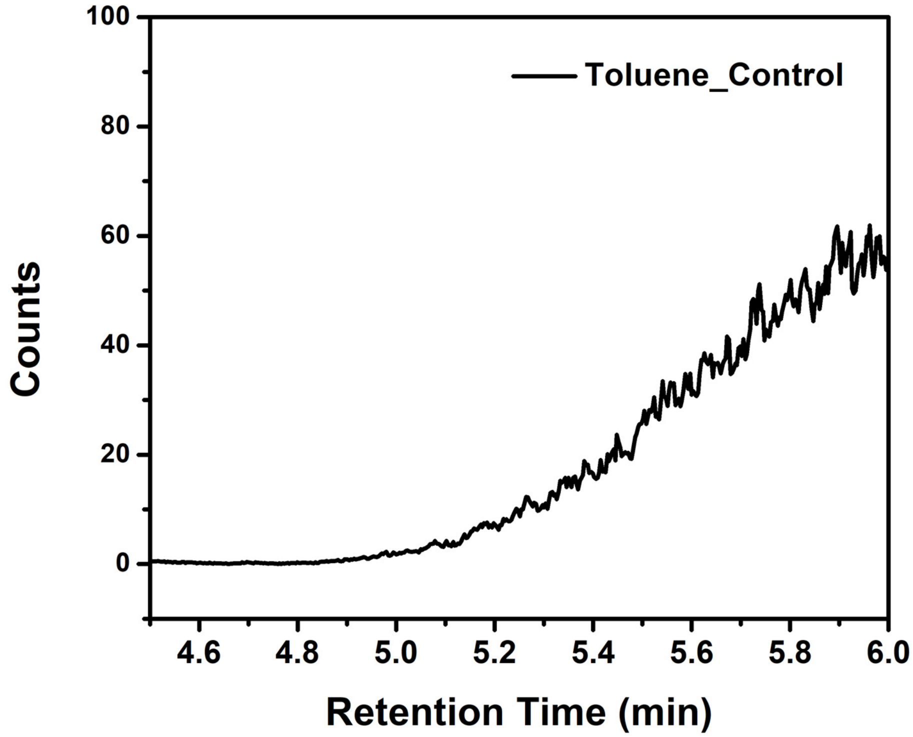

Figure S40. GC trace of the control reaction of toluene heated to 70°C in air for 3 hours

VIII. DFT Calculations

General considerations: Geometry optimization calculations were performed with ORCA software suite using density functional theory (DFT).[8] Geometries were fully optimized starting from coordinates generated from a molecular model built in Avogadro. The B3P functional was used with a basis set of def2-SVP on H, def2-TZVPP on Ni, O, and N, and def2-TZVP on C atoms. The resulting structures were confirmed to be minima on the potential energy surface by frequency calculations using ORCA. Frequency calculations were also conducted using the B3P functional and previously listed basis sets for each atom type. Final spin density plots and Mulliken spin densities were generated from these geometry optimization calculations. Single point broken symmetry calculations using flipspin were also run, but the broken symmetry calculations gave no difference in spin density so those results are not included. Time Dependendent DFT (TDDFT) calculations were undertaken using the PBE0 functional and def2-TZVPP basis set on Ni and def2-TZVP on all other atoms. Furthermore, an effective core potential of SDD was used on Ni. The input file used was the previously optimized geometry for **3** that was optimized using B3P and the previous basis sets.

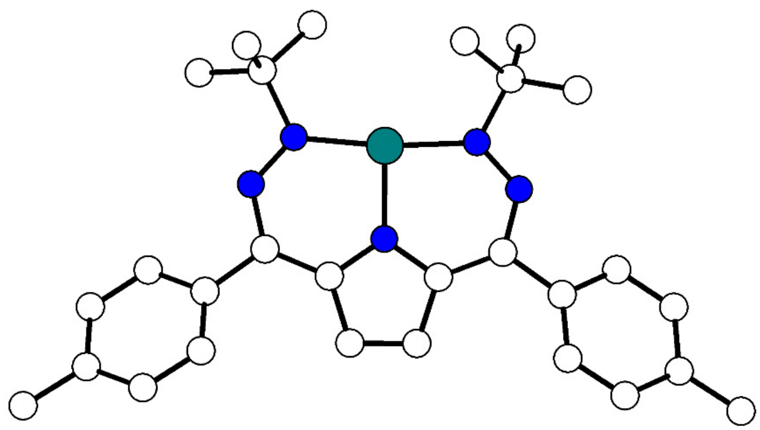

Figure S41. Calculated structure of **1**

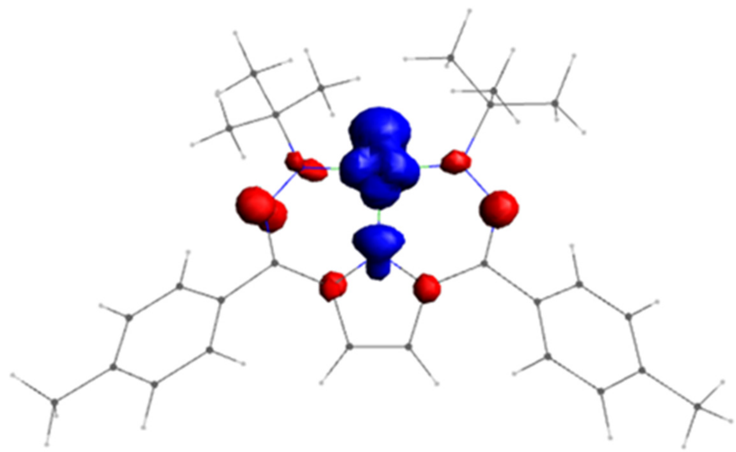

Figure S42. Calculated structure of **1** showing the spin density of the unpaired electron, with iso values set to 0.005

Table S1. Coordinates for the calculated structure of **1**

C	-1.13252322139551	0.76588619144505	-0.00179052748438
C	0.24115790531312	0.76816647670773	0.01003045893462
C	0.66297859626679	2.10800270297869	0.25495659691713
C	-1.56119836316437	2.10810507420334	0.21621632526716
C	-2.87305475220965	2.66017956678554	0.16024836152371
C	1.97617609057733	2.65093185743722	0.30604765476697
C	3.14879708944328	1.79129345412847	0.01223983925147
N	-3.16912326374698	3.94933733763283	0.04261126914468
N	-0.45330924857889	2.88382346278263	0.37212532216143
N	2.30219035421600	3.91509980880582	0.54938823427201
N	1.44289008941987	4.86252518203587	0.78826164247542
N	-2.29615639933584	4.91359286925548	0.03817868096182
Ni	-0.45863418308734	4.75835171611407	0.55755636952991
C	-2.90885431105221	6.24793473711268	-0.21117899287958
C	-4.15137681575656	6.14300886942155	-1.08954715457167
H	-3.92175299620523	5.61111527885107	-2.01766736071197
H	-4.49958996289060	7.14807744764360	-1.34604530347010
H	-4.95498037415075	5.60985982427256	-0.58116670752921
C	2.09382303438402	6.14128204197897	1.18610430185403
C	3.36391377500522	5.89604096011895	1.99744758754720
H	3.15561126334823	5.25683798635180	2.86004396936792
H	3.75419852665772	6.85180338338186	2.36096115548317
H	4.12770691920050	5.40527383641120	1.39432471779228
C	-1.85842001737180	7.08819414377102	-0.93201718903394
H	-1.60881465816724	6.64822613719345	-1.90165005706570
H	-0.93459184508419	7.16552818234958	-0.34485280832555
H	-2.22214323384998	8.10629985148326	-1.09534096952738
C	2.42358469246146	6.94703283869236	-0.07143598754990
H	3.10987528057478	6.38071308934157	-0.70641086125076

H	2.89833511927366	7.89723593598493	0.19344061189350
H	1.52143767373670	7.16591151629517	-0.65140514299065
C	1.08627376730653	6.89167352250071	2.05084459903514
H	1.47507341540870	7.87054195362868	2.34318781131332
H	0.85888849483644	6.32869491064642	2.96157795393418
H	0.14621270549301	7.07408690159295	1.51140982754338
C	-3.26797046944026	6.87981481314948	1.13541077319251
H	-3.98501348216276	6.24780870117207	1.66646008715965
H	-3.71418368410118	7.86961250045973	0.99539935193263
H	-2.38015157071543	6.99731190955840	1.76663212154814
C	3.35624975203286	0.55118824294788	0.61995642152095
C	4.45947190753095	-0.22441230243844	0.29536002459559
C	5.39315155735458	0.20191015729160	-0.64907005295700
C	5.20137883357612	1.45517256547117	-1.22755704152815
C	4.10443128011784	2.23614078114196	-0.90290342457481
C	6.54814705502290	-0.66724407050628	-1.05191684257120
H	7.32377872560986	-0.08705753135339	-1.55846606232055
H	6.21977067293606	-1.45304778656061	-1.74240201477811
H	6.99882246051168	-1.16345137997403	-0.18673240548819
C	-4.18645748680249	0.62014403923967	0.87416710291768
C	-5.34242629274002	-0.15069651604210	0.82296700954555
C	-6.42020502666957	0.20960498503895	0.01957560376258
C	-6.29886655050713	1.37525014371226	-0.74030743787239
C	-5.15132800321632	2.14383841685910	-0.69668352419597
C	-7.67883428757471	-0.60692472260641	-0.02698539494403
H	-7.58259752276628	-1.51946364673380	0.56560690553288
H	-7.92969284454377	-0.89446827498673	-1.05317708688132
H	-8.52885169468630	-0.03897547173457	0.36797098286131
H	-7.12031603042191	1.68475506228946	-1.38238974975413
H	3.97187680859376	3.20735656635316	-1.36740194088453
H	2.65721756732573	0.20024783977533	1.37256467873496
H	4.59883411293197	-1.18235116648666	0.78964531362522
H	5.92258221362343	1.82361825399096	-1.95319538790112
C	-4.06719578703490	1.78483925006322	0.11361940591528
H	-5.07823156473166	3.04483607200089	-1.29447612625257
H	-5.40910456483921	-1.04736704187147	1.43333909283684
H	-3.37968190163305	0.32447275112644	1.53691474105242
H	-1.77767266520601	-0.07774914057912	-0.19485026362163
H	0.89064833574894	-0.07580604910519	-0.16520908878815

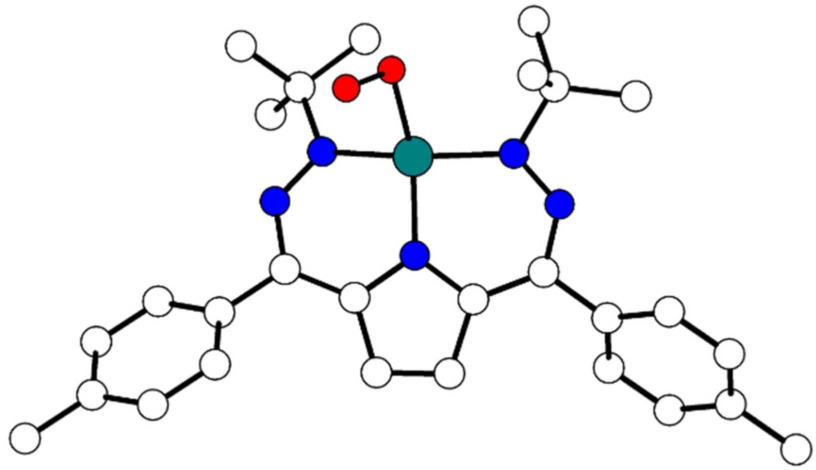

Figure S43. Calculated structure of **3**

Table S2. Coordinates for Calculated Structure of **3**

C	-1.12169265656318	0.85449870271526	-0.06416967432390
C	0.24476172391915	0.83345693607253	-0.12899015175641
C	0.69552738538338	2.20617103673519	-0.05167193792143
C	-1.51918170458032	2.24310929117849	0.04359684836631
C	-2.81344351846670	2.79565773486569	0.05248626631069
C	2.01489850108951	2.68617842682286	0.06327744247487
C	3.19639375010932	1.86890821974831	-0.26831463854705
N	-3.08416478386416	4.10179212434468	-0.16982868226024
N	-0.40096924360202	3.02412928040473	0.05336130600828
N	2.26972373969855	3.88920119665291	0.62657165769039
N	1.41625110211827	4.83712877870317	0.72867205471513
N	-2.21821962155428	5.03849335343823	-0.36815742861305
Ni	-0.31915026253031	4.89321186932138	-0.10258417984563
C	-2.94884437423002	6.35483008484578	-0.70576946796642
C	-4.47161986652610	6.21086000931959	-0.56461472465680
H	-4.88688850110733	5.48437219196748	-1.27334539376472
H	-4.91763592120996	7.19418593175458	-0.77710012831333
H	-4.76559397219641	5.90299491493807	0.44716803651945
C	1.92394874489058	5.92782095718773	1.67502019688013
C	2.51491426074521	5.26907483129894	2.93276055411045
H	1.75847753866423	4.65556985333811	3.44575388627080
H	2.84395289618782	6.05731503343466	3.62579642595902
H	3.37501331928609	4.63407204852731	2.68937396186169

C	-2.63203371953303	6.70344892791627	-2.17078065859405
H	-2.97034794648984	5.89594673194607	-2.83678713029615
H	-1.56505283598440	6.87450455555232	-2.34069573270696
H	-3.17480063914596	7.62074098081222	-2.44619169926302
C	2.99915208187941	6.73485726136902	0.93084356545354
H	3.83809690961721	6.08288969217143	0.65087713595416
H	3.37816401941672	7.53484767373409	1.58536826464419
H	2.59081866420411	7.19160353519259	0.02031637016938
C	0.75582361620541	6.82494269566093	2.09273454074611
H	1.09226035547529	7.49261375611681	2.90006849452309
H	-0.08495924431796	6.22712791235678	2.47514022844384
H	0.40214925922320	7.44951291294405	1.26565597232253
C	-2.48943498353671	7.45290031647577	0.26533857500313
H	-2.67301929886949	7.14847867342605	1.30623940730474
H	-3.07552118441175	8.36402216099658	0.07302451966171
H	-1.43246714876938	7.70678362989809	0.14344360659024
O	0.87006108263291	6.30473908490863	-1.85038803226109
O	0.09410074324592	6.57101810240011	-0.83564458568267
C	3.18810152503754	1.00938331236559	-1.38174956048942
C	4.31066338883608	0.24726591749428	-1.70730615300746
C	5.48575520089989	0.31803337760773	-0.94681167899063
C	5.49762294255635	1.19295161798646	0.15364016386712
C	4.38289224073567	1.95477823031700	0.48739498022278
C	6.69712623266120	-0.50819053245531	-1.29153257124822
C	-4.01948534874774	0.92894241024430	1.24069894535711
C	-5.15934532809898	0.15744354603473	1.45817394586680
C	-6.34095356320083	0.38146378124520	0.73393670728292
C	-6.33548056676334	1.41387293929908	-0.21584392295432
C	-5.19946577688765	2.18926010866753	-0.43926244527787
C	-7.57344865723401	-0.44810663622978	0.98517277395429
H	-7.24069806105476	1.61184172239114	-0.79608198920875
H	4.41447840875300	2.62102691856667	1.35035260925650
H	2.30403598961379	0.96464418871896	-2.02055933181560
H	4.27741835338127	-0.40133708941023	-2.58641992580944
H	6.40136616770367	1.27360749024726	0.76433260885334
C	-4.01229631608591	1.95717499567088	0.27806773756519
H	-5.21850249505007	2.98605231676971	-1.18391060176867
H	-5.13586246925905	-0.62585580507699	2.22106787360346
H	-3.12999257694529	0.75587367761918	1.84964943729700
H	6.55394233007756	-1.05504607976317	-2.23359274040351
H	6.91182553866728	-1.24596772513938	-0.50132868184222
H	7.59386187098743	0.12270161908816	-1.39571526157153
H	-8.38048694858457	-0.18329756724349	0.28838337936188
H	-7.95070792412660	-0.29993815813538	2.01022837772193
H	-7.36303327116620	-1.52354377454909	0.87136283957385
H	-1.79762988621496	0.00583706459690	-0.10615554651696
H	0.89158073300630	-0.03622327842151	-0.19664704009052

Table S3. Orbital Contributions in **1** and **3**

Complex MO	NiL-rad **1** alpha 131	$NiLO_2$ **3** alpha 142
3dz2	0.018358	0.014669
3dxz	-0.02569	0.05018
3dyz	0.013521	0.040462
3dx2y2	-0.13023	0.161115
3dxy	0.006357	-0.03144
4pz	0.010037	-0.01848
4px	0.002705	0.013367
4py	0.075705	-0.01398
% p character	0.088447	-0.0191
% d character	-0.11768	0.234988

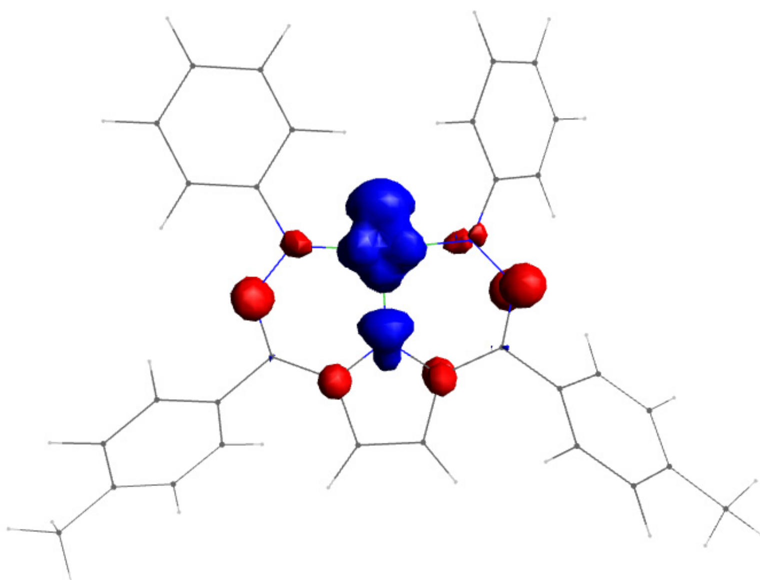

Figure S44. Spin density plot of [^{Ph,Tol}DHP$^{\cdot}$]Ni, with iso values set to 0.005

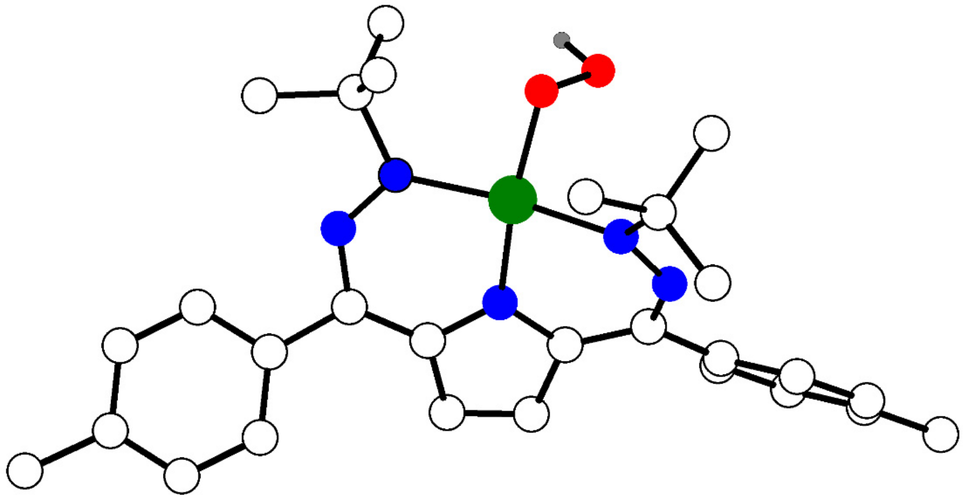

Figure S45. Calculated Structure of [^{tBu,Tol}DHP]NiOOH

Table S4. Coordinates of calculated structure of [^{tBu,Tol}DHP]NiOOH

C	-1.10533597856450	0.78240898942854	0.05737356014129
C	0.24626869895660	0.75992433794550	-0.02331750186244
C	0.69688451341491	2.13224046795793	0.02576035358750
C	-1.50124297695312	2.17390133827943	0.12295668110518
C	-2.78159621701123	2.71915646126632	0.06889221725178
C	2.00048374213627	2.60450695160969	0.12146044246700
C	3.20086266131919	1.83532667484701	-0.22470607201949
N	-3.02848912753031	4.00994392603471	-0.22951824114925
N	-0.39171648505275	2.94884942703255	0.12460105674850
N	2.25229565630367	3.80425425891136	0.69520500089568
N	1.41921307005062	4.73700153314167	0.79590253078582
N	-2.17271329488539	4.92425296249491	-0.43523796422343
Ni	-0.29778483468470	4.80452521662750	-0.04588150143092
C	-2.88298856554647	6.21534931498631	-0.81804306373019
C	-4.39462661187235	6.01995013149489	-0.90578548968033
H	-4.66482374387236	5.28563010484751	-1.66665757054762
H	-4.83500016001761	6.98049561727851	-1.19055932196112
H	-4.82898954704726	5.69864036692084	0.04200939884370
C	1.92554880174786	5.82776416490166	1.71720594766153
C	2.81258810794172	5.22511611334852	2.80591012443812
H	2.29782696840579	4.42051579792887	3.34015120174814
H	3.05452223230989	6.01357605910715	3.52423296056323
H	3.74538863891915	4.83278887163010	2.40103757235474
C	-2.39838542663018	6.65156142996395	-2.20281514189267
H	-2.49350430450228	5.82671332863385	-2.91584062044706

H	-1.36841504996643	6.99823387330298	-2.16488776152532
H	-3.02441109019812	7.47465388180906	-2.55872369023991
C	2.73533838211551	6.82603569996736	0.89127848439795
H	3.54593577184513	6.31134212592382	0.36830233554858
H	3.17609459392220	7.56812225963577	1.56502427348587
H	2.10367391800669	7.32887525955476	0.16029102986018
C	0.72652214038603	6.49340746501797	2.37741660387065
H	1.08446466226688	7.23761670720722	3.09501442396541
H	0.12338031566168	5.76004692359217	2.92339987704064
H	0.10367375419614	7.00080321322899	1.64236871119493
C	-2.60032951787875	7.26439445836273	0.25696989957324
H	-2.94637170890227	6.90561560157157	1.23144270782377
H	-3.15406660194006	8.17801618420464	0.01906138590345
H	-1.54162085388009	7.51381684882796	0.31410287839134
O	1.00669584633509	6.25861652715745	-1.67362979600675
O	0.06903220823822	6.52157046642981	-0.61032565672858
C	3.22737254320305	0.98151070346160	-1.33117485177389
C	4.39839752075106	0.33527461399055	-1.70143654772678
C	5.58184249681877	0.51924367599836	-0.98918676053601
C	5.55129810174589	1.37397807609420	0.11445530471220
C	4.39054027970866	2.02093247264303	0.49116363488313
C	6.85080319228125	-0.18131363968506	-1.37382537078497
C	-4.11853834551087	0.93468043857427	1.24926993429851
C	-5.32809690161776	0.29666622290934	1.48389974420092
C	-6.47756717655193	0.63491203913844	0.76854297568656
C	-6.36514724034731	1.61891497405499	-0.21087951082947
C	-5.16214326304615	2.25574863333293	-0.45269480502369
C	-7.80239881066887	-0.00665226691982	1.05253982202677
H	-7.24348396181128	1.90277530089194	-0.78413739839731
H	4.39157894255751	2.68645278963965	1.34639338176578
H	2.33458888389347	0.85959876319727	-1.93660706155097
H	4.39501493055369	-0.30471471086553	-2.57988685195509
H	6.46220435033600	1.54124966044019	0.68339568896731
C	-4.01395840354229	1.93576396119216	0.27746449595570
H	-5.10313360562586	3.03089652019585	-1.20692216757746
H	-5.38504959023671	-0.45883699782926	2.26412342241456
H	-3.25834754547831	0.68595256134825	1.86326019955246
H	6.82330059945726	-0.52053637455211	-2.41237343304777
H	7.01710558593324	-1.06208358861131	-0.74389567771401
H	7.71633718039863	0.47595256809277	-1.24692438452316
H	-8.59410217268556	0.45409043990293	0.45849787688935
H	-8.07111863785816	0.09846014916117	2.10962284311898
H	-7.78905892685647	-1.07771024429906	0.81962604535656
H	-1.78079974900093	-0.06010671501975	0.04834318667250
H	0.89191429502524	-0.10432706253213	-0.07936173622758
H	0.43773284063170	6.29847569364061	-2.46087426503630

Table S5. Tabulated energies for calculation of O-H BDE

	$NiLOO^{\cdot}$ (**3**)	TEMPOH	→	NiLOOH	TEMPO	Reaction Energy	O-H BDE = Reaction energy – 70 kcal/mol (TEMPOH BDE[7])
Energy (hartrees)	-3019.54	-484.133		-3020.15	-483.53	.011	0.10
Energy (kcal/mol)	-1894761.35	-303793.45		-1895144.12	-303415.07	-7.25	63

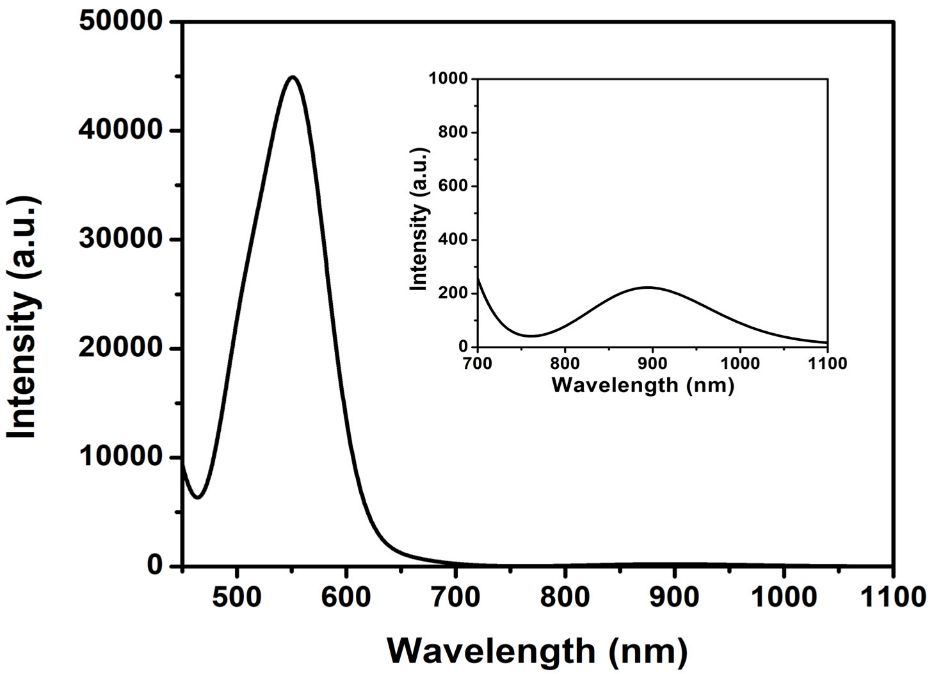

Figure S46. TD-DFT predicted UV-vis spectrum of **3**. 2000 cm^{-1} line broadening was applied. Inset shows the low-energy feature.

Table S6. Wavelength and intensities of transitions of **3** calculated by TD-DFT.

Wavelength (nm)	Intensity (au)
933.6196	9.1903
911.1119	70.896
885.3161	146.0343
766.2071	10.2842
647.5551	474.347
626.8452	409.527
620.5321	12.011
557.5503	38981.518
531.6914	3904.827
513.9327	1174.971
510.1364	15775.096
501.4693	1577.0208
492.1235	1691.643
488.7370	133.889
478.2812	1420.766
444.0261	1585.1
439.5624	2018.025
432.1465	2132.674
431.4194	7024.7875
417.765	2626.557
410.3254	284.9424
408.8976	4827.142

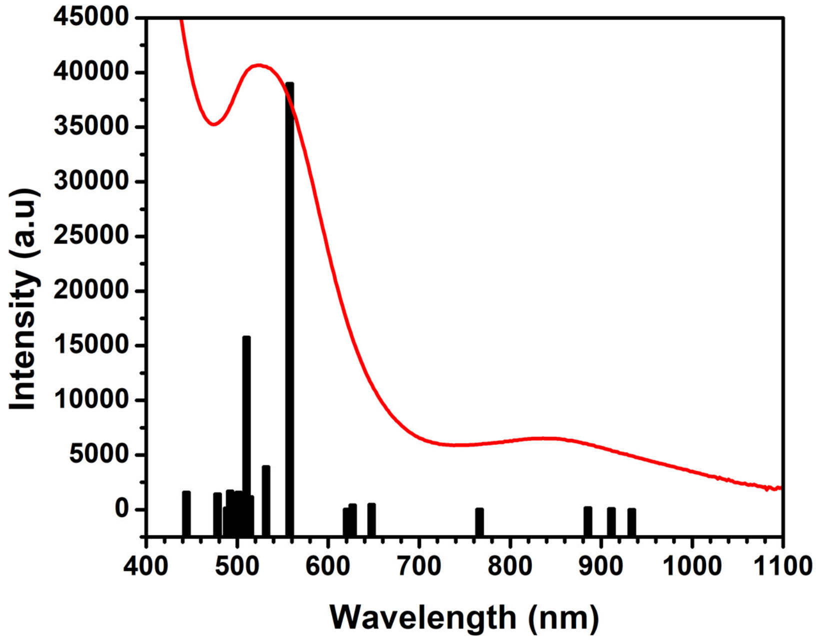

Figure S47. TD-DFT calculated UV-vis transitions of and the experimental collected UV-vis of **3** (red)

IX. X-ray Absorption Studies

EXAFS fit of Complex 3

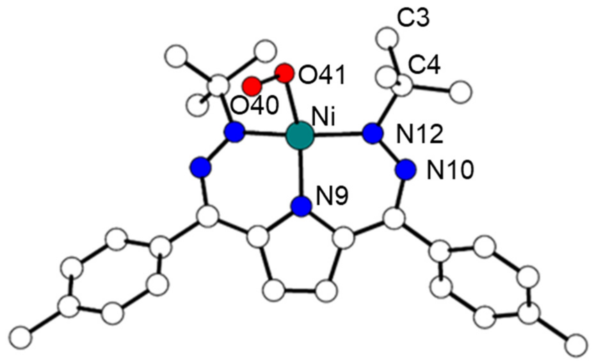

Figure S48. Calculated structure of **3** with atom labels.

Table S7. EXAFS Fit Parameters for **3**

Complex **3**	N	R (Å)	σ^2 (Å^2)	R-factor	Reduced chi-square
Ni-N9	1	1.873(6)	0.0022(9)	0.0080	20.6
Ni-N12	2	1.920(6)	0.0022(9)		
Ni-O41	1	2.08(1)	0.0009(5)		
Ni-O40	1	2.70(1)	0.0009(5)		
Ni-N10	2	2.870(6)	0.0022(9)		
Ni-C3	1	3.05(3)	0.009(4)		
Ni-C4	1	3.09(3)	0.009(4)		

ΔE_0 = -2.4 eV; S_0^2 = 0.74; Independent Points: 13.9; Fitting Range: k: 1-11.5 Å^{-1}; R: 1.0-3.1 Å
N, Coordination numbers; R, interatomic distances; σ^2, Debye-Waller factors (the mean-square deviations in interatomic distance). The values in parentheses are the estimated standard deviations; ΔE_0, change in the photoelectron energy; S_0^2, amplitude reduction factor.

Table S8. Comparison of EXAFS and DFT calculated bond lengths of **3**

Complex **3**	N	DFT model	XAFS R (Å)
Ni-N9	1	1.8770	1.873(6)
Ni-N12	2	1.8774	1.920(6)
Ni-O41	1	1.9241	2.08(1)
Ni-O40	1	2.5420	2.70(1)
Ni-N10	2	2.8739	2.870(6)
Ni-C3	1	2.8727	3.05(3)
Ni-C4	1	2.9128	3.09(3)

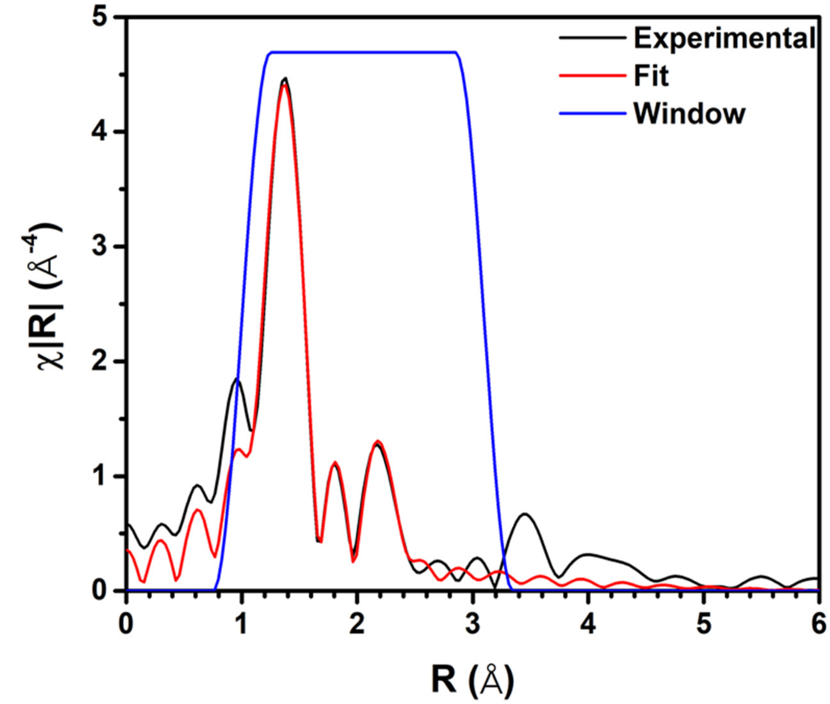

Figure S49. EXAFS spectrum (black) and fits (red) in R-space at the Ni K-edge absorption of **3**

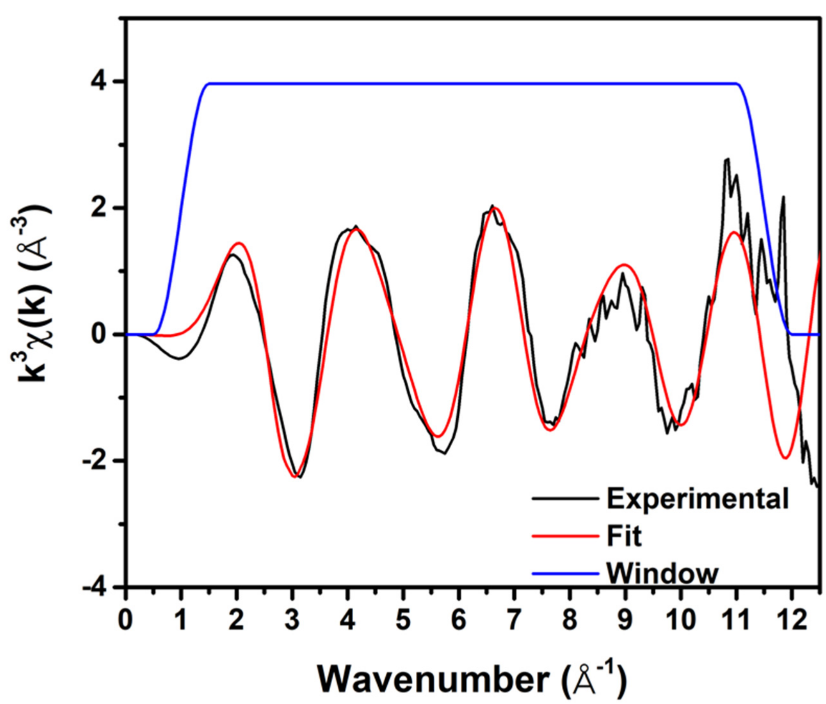

Figure S50. EXAFS spectrum (black) and fits (red) in k-space at the Ni K-edge absorption of **3**

EXAFS fits with/without O40 atom

Table S9. XAFS fit parameters of pathways with or without O40 (second O)

Fit parameters		**ON_3C_2O**	**ON_3C_2**
O41	ΔR(Å)	0.20(1)	0.20(3)
	σ^2 (Å^2)	0.0005(9)	**-0.001(3)**
N	ΔR(Å)	-0.004(6)	-0.002(3)
	σ^2 (Å^2)	0.0022(9)	0.002(2)
C	ΔR(Å)	0.18(3)	0.20(4)
	σ^2 (Å^2)	0.009(4)	0.002(5)
O40	ΔR(Å)	0.16(1)	
	σ^2 (Å^2)	0.0009(5)	
ΔE_0 (eV)		-1.4(8)	0(2)
S_0^2		0.74(8)	0.7(2)
R-factor		0.0080	**0.0747**
Reduced chi-square		20.6	160.2

Independent Points: 13.9; Fitting Range: k: 1-11.5 Å^{-1}; R: 1.0-3.1 Å

X. X-ray Crystallography

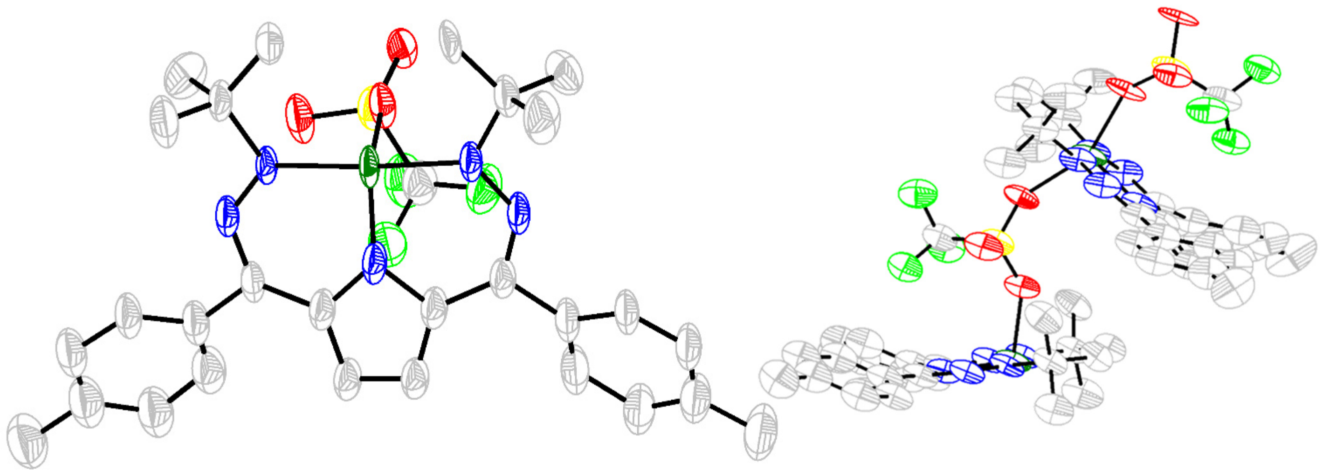

Figure S51. Solid state structure of **3**, with triflate bridging to form 1D chains

Table S10. Crystal data and structure refinement for (1) and (2).

Identification code	(1)	(2)
Empirical formula	$C_{28}H_{34}N_5Ni$	$C_{58}H_{68}F_6N_{10}Ni_2O_6S_2$
Formula weight	499.31	1296.76
Temperature/K	100(2)	100(2)
Crystal system	monoclinic	Triclinic
Space group	C2/c	P-1
a/Å	51.354(6)	12.197(6)
b/Å	5.7125(7)	15.166(8)
c/Å	17.328(2)	21.970(11)
α/°	90	71.701(12)
β/°	93.198(4)	76.170(11)
γ/°	90	69.672(13)
Volume/Å^3	5075.5(10)	3579(3)
Z	8	2
ρ_{calc}g/cm^3	1.307	1.203
μ/mm^{-1}	0.790	0.649
F(000)	2120.0	1352.0
Crystal size/mm^3	0.36 × 0.21 × 0.17	0.36 x 0.24 x 0.22
Radiation	MoKα (λ = 0.71073)	MoKα (λ = 0.71073

2Θ range for data collection/°	4.708 to 50.328	4.292 to 37.618
Index ranges	$-60 \le h \le 59$, $-6 \le k \le 6$, $-20 \le l \le 20$	$-10 \le h \le 11$, $-13 \le k \le 13$, $-19 \le l \le 19$
Reflections collected	40928	18028
Independent reflections	4486 [R_{int} = 0.0850, R_{sigma} = 0.0449]	5349 [R_{int} = 0.0758, R_{sigma} = 0.0739]
Data/restraints/parameters	4486/351/407	5349/1703/883
Goodness-of-fit on F^2	1.078	1.045
Final R indexes [I>=2σ (I)]	R_1 = 0.0672, wR_2 = 0.1602	R_1 = 0.1592, wR_2 = 0.3329
Final R indexes [all data]	R_1 = 0.0851, wR_2 = 0.1703	R_1 = 0.1917, wR_2 = 0.3534
Largest diff. peak/hole / e $Å^{-3}$	0.72/-0.76	1.48/-0.99

XI. References

1. Stoll, S.; Schweiger, A., Easyspin, a Comprehensive Software Package for Spectral Simulation and Analysis in EPR. *J. Magn. Reson*. **2006**, *178*, 42

2. Sheldrick, G. M. SHELXT- Integrated space-group and crystal-structure determination. *Acta Cryst***. 2015**, *A71*, 3-9

3. Dolomanov, O.V.; Bourhis, L. J.; Gildea, R. J.; Howard, A. K.; and Puschmann, H.,. Olex2, a complete structure solution, refinement, and analysis program. *J. Appl. Cryst*. **2009**. *42*, 339

4. (a) Sheldrick, G. M. A Short History of SHELX. *Acta Cryst*. **2008***, A64*, 112-122; (b) Sheldrick, G. M. Crystal structure refinement with SHELXL. *Acta Cryst*. **2015,** *C71*, 3-8

5. (a) Ravel, B., Newville, M., ATHENA, ARTEMIS, HEPHAESTUS: data analysis for X-ray absorption spectroscopy using IFEFFIT. *J. Synchr. Radn*., **2005**, *12*, 537-541 (b) Newville, M., IFEFFIT: interactive EXAFS analysis and FEFF fitting. *J. Synchr. Radn*. **2001**, *8*, 322-324; (c) Rehr, J. J.; Albers, R. C. *Rev. Mod. Phys*. **2000**, *72*, 621-654.

6. (a) M.-C. Chang, A. J. McNeece, E. A. Hill, A. S. Filatov, J. S. Anderson, *Chem. - Eur. J.* **2018**, *24* (31), 8001-8008. (b) A. J. McNeece, M.-C. Chang, A. S. Filatov, J. S. Anderson, *Inorg. Chem.*, **2018**, *57*, 7044-7050.

7. Y.-R. Luo, *Handbook of Bond Dissociation Energy in Organic Compounds.* CRC Press, **2002**.

8. Neese, F. "The Orca Program System" *Wiley Interdisciplinary Reviews: Computational Molecular Science* **2012**, *2*, 73-78. H - Kr: Schaefer, A.; Horn H.; Ahlrichs, R. *J. Chem. Phys*. **1992**, *97*, 2571. Rb - Xe: Schaefer, A.; Huber, C.; Ahlrichs, R. *J. Chem. Phys*. **1994** *100*, 5829; Weigend, F.; Ahlrichs, R. *Phys. Chem. Chem. Phys*. **2005**, *7*, 3297.